Sādhanā (2026) 51:12
https://doi.org/10.1007/s12046-025-02997-3

Investigation of the machining, structural and antibacterial properties on Ti6Al4V alloy by PMEDM: Taguchi optimizing the influence of HA, hBN and HA/hBN doping

LEVENT URTEKIN[1], FAIK YILAN[1,*], IBRAHIM BAKI ŞAHIN[1], TALIP CEYHAN[1], ALI SEVIM[2] and ASIM GENÇ[3]

[1]Department of Mechanical Engineering, Faculty of Engineering-Architecture, Kırsehir Ahi Evran University, 40100 Kırsehir, Turkey
[2]Department of Genetic and Bioengineering, Faculty of Engineering-Architecture, Kırsehir Ahi Evran University, 40100 Kırsehir, Turkey
[3]Department of Machinery and Metal Technology, Gazi University, 06000 Ankara, Turkey
e-mail: faik.yilan@ahievran.edu.tr

MS received 29 August 2024; revised 20 June 2025; accepted 17 July 2025

Abstract. This study systematically investigates the individual and combined effects of hydroxyapatite (HA) and hexagonal boron nitride (hBN) nanopowders as dielectric additives during PMEDM processing of Ti6Al4V alloys, providing comparative insights into their influence on surface integrity, mechanical performance, and antibacterial properties. In this context, X-ray diffraction (XRD), optical and scanning electron microscopy (SEM), energy dispersive spectrometry (EDS), surface roughness (SR), contact angle measurements were used to characterize the structural and morphological properties of the samples on the surface and subsurface. Powder additives were deposited onto the surfaces of the samples using different processing parameters during the EDM process, and XRD and EDS results revealed the presence of HA and hBN phases. In this regard, the surface roughness values varied between 2.03 μm and 3.97 μm on average, depending on the discharge current, pulse duration and the different powder ratios added to the dielectric liquid. In addition, while the cratered structures formed on the surfaces of the samples processed after EDM reduce the surface wettability, the best wettability was observed on the surface processed with a discharge current of 9 A, a pulse duration of 200 μs, and the addition of 15 g/l hydroxyapatite (HA) powder. In order to correlate processing performance with the effect of added dust concentrations on biofilm, cellular adhesion and proliferation were examined with *Staphylococcus aureus* bacterial strain at 2, 4, and 6 h. This showed that a 5 g powder additive promoted cellular activity growth, while a 10 g concentration inhibited it, except for HA/hBN particles. Extending exposure to 15 g further confirmed biofilm formation, highlighting the complexity of bacteria adhesion.

Keywords. Titanium and alloys; powder-mixed electrical discharge; taguchi design; hydroxyapatite; hexagonal boron nitride; bacteria adhesion.

1. Introduction

Titanium is widely used for implants because of its high corrosion resistance, low weight, strength, heat resistance, and stability. Its excellent biocompatibility makes it suitable for medical devices like artificial hearts, bone plates, joints, and dental implants. However, titanium alloys are bioinert and cannot form strong chemical bonds with bone, which is a limitation for ideal biomaterials [1–6]. These materials do not possess all the characteristics of an ideal biomaterial, as they are bioinert and cannot form a strong chemical bond with bone. For bone bonding, the initial development of apatite is essential. However, titanium, vanadium, and aluminum ions released from Ti6Al4V alloy may inhibit this process [7, 8]. Therefore, using powder-mixed electrical discharge machining (PMEDM) can enhance the processing performance and biocompatibility of titanium alloys by providing the required surface integrity for implant applications [9–11]. Thus, an unconventional manufacturing method stands out in terms of both surface shaping and a coating for healthcare applications [12].

PMEDM is a unique EDM technique that involves mixing metallic powders with dielectric liquid to enhance the quality of machined surfaces and overall machining efficiency [13]. In addition, electrically conductive powder

*For correspondence
Published online: 05 January 2026

additions extend the discharge range, improving the precision and machined surface quality of the machining process [14, 15]. By applying appropriate powder additives to the machined surface, it is possible to create a lubricating layer, improve the surface's resistance to corrosion, and noticeably increase its hardness in comparison to the anaphase material [16]. Numerous powder particles, including Al_2O_3, SiC, Zn, hydroxyapatite (HA), and hBN, were added to the EDM dielectric to significantly increase process output variables and modify the surface of biomaterials[17–19]. Despite encouraging reports, appropriate machining selection remains challenging; selection depends on a variety of factors, including surface treatment effectiveness, powder used, parameters, cost, and limitations based on material and part geometry.

Different studies have been carried out to examine the effects of processing with n-HA and hBN powder additives added to the dielectric fluid in PMEDM on the mechanical, tribological and biological properties of titanium alloys [20–23]. Öpöz et al. [24] indicated that n-HA mixed EDM was used to investigated its surface formation characteristics and in vitro osteoblast-like MG-63 cell response. The surfaces showed higher surface roughness and hydrophilic properties, promoting cellular activity and biocompatibility. The n-HA mixed EDM also improved cell attachment and growth. Singh Bains et al. [25] examined the impact of n-HA powder-mixed dielectric and machining input factors on output factors like MER and SR, as well as wear rate and corrosion behavior in implant materials. Results showed that hole diameter, peak current, dielectric fluid type, and pulse-on time significantly influenced MER and SR, while n-HA powder on Ti6Al4V showed lower corrosion and wear rates. Nauryz et al. [26] examined the performance of HA PMEDM on Ti6Al4V alloy and its impact on antibacterial properties. This study examined the machining performance metrics, including surface roughness, contact angle, and antibacterial properties. The results showed a correlation between discharge energy and powder concentration with antibacterial properties. The modified surfaces reduced biofilm formation under low discharge energy and a 0.273 μm roughness, suggesting that roughness can optimize surface antibacterial properties. Saurabh et al. [27] suggested using graphite nanopowder mixed electric discharge machining (NPMEDM) for machining Ti6Al4V using deionized water as a dielectric. Comparing conventional EDM and NPMEDM processes, the study found that the addition of nano graphite powder improved surface integrity, recast layer thickness, material removal rate, chemical analysis, and residual stress. The addition of graphite powder also led to a 69% improvement in recast layer thickness and a 74.75% improvement in surface roughness compared to conventional EDM. The induced residual stress was also significantly improved, reducing component failure risk. In another study, Sharma et al. [28] investigated the application of a hard, wear, and corrosion resistance coating on titanium alloy using hexagonal boron nitride powder suspended in deionized water. The coating's surface exhibits phases like BN, Al_2O_3, TiN, TiAlN, TiO, and CuO. The coating's micro-hardness increases is five times higher than that of the parent material. Pin on disk wear tests show a reduction in wear rate and improved corrosion resistance. On the other hand, Devgan and Sidhu [29] explored that the use of Electro Discharge Treatment (EDT) to modify the surface of β-type titanium substrate using multi-walled carbon nanotubes (MWCNTs) and μ-hydroxyapatite powders in a dielectric medium. The L18 array was used to analyze the surface's cell viability, revealing that MWCNTs promote cell proliferation. The treatment also enhanced porosity, making it suitable for bone grafting. X-ray patterns showed the formation of biocompatible phases. The positive polarity of the graphite tool electrode was the most desirable process parameter. Recent studies have separately highlighted the potential of hydroxyapatite (HA), known for its osteoconductivity, and hexagonal boron nitride (hBN), recognized for its mechanical reinforcement and anti-bacterial properties, as promising candidates for surface modification. However, there is a notable gap in the literature regarding the combined use of HA and hBN as powder additives in powder-mixed electrical discharge machining (PMEDM), particularly in terms of their synergistic effects on both surface integrity and biological performance of titanium alloys.

As researched in the literature, it has been observed that detailed results regarding the effects of HA, hBN and HA/hBN combination at different powder ratios that were added into the dielectric liquid of Ti6Al4V alloy with PMEDM on surface integrity and machining performances as well as cellular activity (biofilm) performances have not been presented. To our knowledge, there is no study in the scientific literature yet that examines the optimal conditions for cell adhesion, bacterial proliferation and differentiation on Ti6Al4V alloy surfaces by adding HA, hBN and HA/hBN additive nanopowders during PMEDM. Therefore, in this study, an L9 Taguchi orthogonal array was designed and applied on titanium alloys, taking into account the discharge current, discharge time, and concentrations of HA, hBN, and HA/hBN nanopowder particles. For this research, the structural and morphological characterizations of the additive powders deposited on the surfaces of the samples with PMEDM were investigated using X-ray diffraction (XRD), scanning electron microscopy (SEM), energy dispersive spectroscopy (EDS), surface roughness (SR) and contact angle device. In addition, their cell proliferation tests were examined by using Staphylococcus aureus (S. aureus).

2. Materials and methods

2.1 *Materials and EDM process*

In this study, Ti6Al4V alloys as workpieces were cut with a laser cutting machine in the form of 20 × 20 × 2 mm^3 rectangular plates. The chemical composition of the workpiece by weight is 89.36Ti-5.77Al-4.86V. Before PMEDM processes, each sample was polished with SiC abrasives from 80 to 1200 mesh, followed by final surface polishing with 3 μm diameter alumina powder. Then, the copper tool with the highest electrical conductivity and 99.99% purity was used as the electrode. Here, the physical properties of copper electrode density are 8.904 g/cm^3, melting point is 1083 °C and boiling point is 2580 °C. The detailed information about the machining processes can be found in a different study, which has been performed by one of the authors of the present study [30].

Hydroxyapatite (HA) powder used in the dielectric fluid was sourced from KuantaMET Medikal, while hexagonal boron nitride (hBN) powder was purchased from Bortek Boron Technologies. The mean particle sizes were 26 nm for HA and 70 nm for hBN. The nano powder-assisted EDM was performed on a FURKAN "K1 Z-NC" machine at Gazi University. The standard dielectric system was removed and replaced with a small, custom system consisting of a plastic chamber, sample holder, tool holder, and mechanical mixer. The workpiece was connected electrically via a stainless steel holder with liquid-tight gaskets. This setup allowed for efficient use of small amounts of dielectric liquid and powder, and made the process cleaner, safer, and more controlled. Figure 1 shows the test system of the PMEDM process.

The HA, hBN, and HA/hBN powders were carefully weighed with a precision balance (0.01 g accuracy) and added to deionized water to prepare the dielectric liquid. To achieve a uniform distribution of the HA, hBN, and HA/hBN powders in the deionized water and to maintain the dielectric liquid at a suitable temperature, the dielectric tank was continuously mixed at a constant speed both before and during the process. A mechanical mixer rotating at 1500 rpm was utilized for this purpose. This mixing process ensures that the additives are evenly dispersed in the liquid and helps in cooling the dielectric fluid during the operation.

2.2 *Experimental model employing Taguchi's method*

Design of Experiments (DOE) is a strategic method for obtaining statistically meaningful data with minimal experimental effort. The Taguchi method, in particular, is systematic: it starts by defining the objective or response variable, then identifying factors that may affect it, and assigning levels to these factors. An orthogonal array is used to determine the effect of each factor efficiently [31]. The process culminates in the determination of the most favorable factor levels to optimize the response variable. The Taguchi robust parameter design method is recognized for its effectiveness in experimental design and optimization processes. It has gained considerable application in enhancing offline quality control measures [32, 33]. Central to the Taguchi method is the utilization of specially designed orthogonal arrays, which facilitate the analysis of the entire parameter space with a minimal experimental set. These arrays, structured with numbers in rows and columns, enable the identification of optimal parameter levels for a given response variable by representing the factor levels in each experiment (rows) and their impact on the response (columns) [34, 35]. This design allows for the selection of the most suitable orthogonal array based on the factor levels involved. Taguchi L9 orthogonal array, encompassing three levels for two factors, was employed in the experimental setup as depicted in Table 1. The selection of factors and their respective levels was guided by findings from existing literature [30, 36–38].

2.3 *Characterizations*

Phase analysis and crystallographic structures of the samples processed with HA/hBN powder additive at different parameters were performed with a Panalytical brand/Axios MAX model X-ray diffractometer device. XRD analysis was analyzed under the condition of scan range (2θ) 20°–70° and Cu-Kα radiation (30kV, 15mA). Surface images and quantitative chemical analyzes of PMEDM samples were carried out by scanning electron microscopy (FE-SEM/EDS). Measurement of average surface roughness on the samples was carried out with the Mahr Marsurf PS 10 portable surface roughness device. While measuring the average surface roughness, three measurements were made from random areas in the machining direction and the average surface roughness value was obtained by averaging these values. The contact angle measuring (ATM) instrument utilized was the Attension Theta Flex type manufactured by Biolin Scientific. A total of 5μl of distilled water was used for the measurements, which were taken at room temperature over a 10-second interval.

2.4 *Bioactivity test solutions*

Staphylococcus aureus strain ATCC 25923, which is known to have biofilm forming ability, was taken from stock culture and streaked on trypticase soy agar (TSA) medium. The next day, a single colony was selected and inoculated into sterile 3 ml of trypticase soy broth (TSB) and grown at 37°C for 18 hours. After that, 1 ml of the culture was diluted with sterile TSB at a ratio of 1:10 and left to incubate at 37°C for 3 hours to obtain active growing

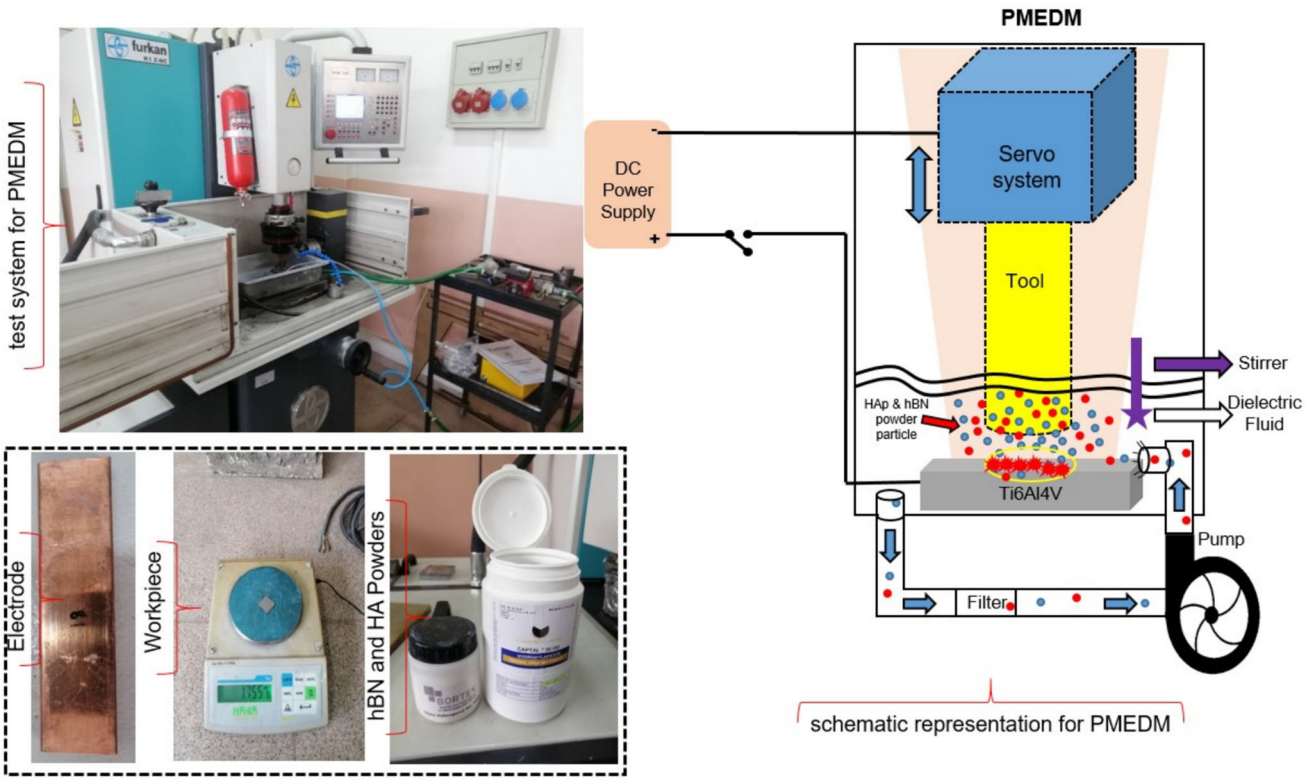

Figure 1.. Schematic illustration of the custom PMEDM test system, including the plastic processing chamber, sample and tool holders, mechanical mixer, and the flow/circulation of the powder-mixed dielectric liquid used for machining Ti6Al4V alloys with HA/hBN additives.

Table 1. Taguchi L9 orthogonal array

#run	Discharge current, I_p (A)	Pulse on time, t_{on} (μs)	Deionized water+(HA-hBN- HA/hBN) (g/l)
1	9	100	5
2	9	150	10
3	9	200	15
4	12	100	10
5	12	150	15
6	12	200	5
7	15	100	15
8	15	150	5
9	15	200	10

bacterial cells (logarithmic cells). At the end of incubation, the culture was centrifuged at 4,000 g for 10 min and the cells that settled to the bottom were suspended in 5 ml of sterile phosphate saline buffer (PBS). The cell concentration was adjusted with a spectrophotometer to be 1×10^5 cfu/ml (optical density $(OD)_{600} = 0.2$) and was used directly in biofilm experiments [39, 40].

Test specimens were first subjected to surface sterilization with UV light for 1 h and then sterilized in an autoclave at 121°C at 1.1 atm pressure for 15 minutes. Then, 200 μl of the bacterial suspension prepared as described above was dropped onto each sample surface and left to incubate at room temperature for 1 hour. The test specimens were then gently washed 2 times in sterile PBS to remove non-adherent and loosely adherent bacterial cells. Finally, the test specimens were transferred to sterile TSB and incubated at 37°C for 2h, 4h and 6h, respectively, to form bacterial biofilm on the test surfaces [39, 40]. All experiments were carried out in three repetitions. At the end of all three incubation periods, the test samples were removed from the TSB, the excess media were removed by tapping and dried in a sterile cabinet. Then, the bacteria on the surface were fixed with methanol and dried at room temperature. Finally, the samples were stained with 0.5% crystal violet and examined under a microscope. The horizontal biofilm formation on each test specimen was examined using an optical microscope at a magnification of 600× (AOB&OPTİMUS, New Taipei City, Taiwan). For the three-repeated experiments, a total of 3 images from each sample were taken with an optical cameSR (TOUPCAM, Zhejiang, China). In total, 9 images were obtained for a test sample. The obtained images were converted to gray format with the ImageJ 1.54g program and analysed. The numerical data obtained were determined as percent

biofilm coverage ratio (BCR). Bacterial films that adhered and reproduced on the surface of the test samples were calculated as the percentage coverage rate according to the total area ratio. Analysis of variance (one-way ANOVA) was used to compare the test samples with respect to BCR using percent data. Samples for 2h, 4h and 6h incubation periods were separately compared. LSD multiple comparison test as post-hoc was used for all pairwise comparisons. All data were tested with respect to variance homogeneity using Levene statistics, and all percentage data were subjected to arcsine transformation to stabilize variances before statistical analysis. p-value less than 0.05 was considered as statistically significant.

3. Results and discussion

3.1 *Structural examinations*

XRD graphs of the samples processed by adding HA, hBN and HA/hBN nano powders in different concentrations to the dielectric liquid are given in figure 2. Both α-Ti and β-Ti phases were obtained from the substrate, as expected from its material. confirmed the formation of TiO by chemically bonding to oxygen atoms during PMEDM. When the XRD patterns were examined, the presence of HA, hBN and HA/hBN nanopowders participating in the processing of the surfaces of Ti6Al4V alloy samples was observed with decreasing/increasing peak intensities at different diffraction angles. In hBN samples, the intensity of BN phases corresponding to the diffraction peaks at 2 θ = 27,2°, 36°, 43,6°, 57,8° is considerably higher than the HA reflection peaks coming from the HA-doped sample.

Surface SEM images of HA, hBN and HA/hBN added samples are given in figure 3. Current intensity, discharge time and nanopowder amount parameters during the EDM processing mechanism affect the sample surfaces. When SEM images were examined, it is seen that the formation of some micropore, microcracks and shallow craters commonly seen in PMEDM. The reason for this is confirmed by the theory of multiple sparks and discharge gap expansion in relevant literature studies [41, 42]. Additionally, when the surface were examined, it is seen that there is sufficient adhesion at varying thicknesses depending on the nanopowder material. Meanwhile, agglomerations became more evident in the hBN samples with increasing current intensity. As a result, the bumps and protrusions formed on the surfaces of these samples caused the surface roughness to increase.

SEM surface graphs and EDS spectra of the samples are given in figure 4. Chemically represented elements of $Ca_{10}(PO_4)_6O_2$ HA nanopowder content were detected in all processing results. On the other hand, the electrode used is observed on the machining surface. Accordingly, in addition to workpiece components such as Ti, Al, V, Ca and P elements were detected on the surfaces processed by HA-doped EDM. According to the EDS results obtained from hBN surfaces, it confirmed the presence of N and B. In the light of this information, the amount of elements varies according to the weight ratio in HA/hBN added samples under each processing condition. The SEM surface graphs and EDS spectra of the samples are given in Figure 4. As can be seen from the SEM image of the HA added sample, the elements of the chemically represented $Ca_{10}(PO_4)_6O_2$ HA nanopowder content are clearly seen in all processing results. Accordingly, in addition to the workpiece components such as Ti, Al, V, Ca and P, elements were detected on the surfaces processed with HA added EDM. According to the EDS results obtained from hBN surfaces, the presence of N and B was confirmed. In the light of this information, the amount of elements in the samples of the three HA/hBN added nanoparticles in each machining processing condition varies according to the weight ratio. In particular, the copper electrode used was observed on the processing surface. In addition, when cross-sectional SEM images, SEM and EDS images are examined together, it is seen that the oxygen released during the discharge forms porous structures as expected from the PMEDM process. The formation of micropores is consistent with previous studies [25, 43].

Table 2 shows the surface roughness results of the EDM process performance of the nanopowder added Ti6Al4V alloy. Different concentrations of HA, hBN and HA/hBN nanopowder added to the dielectric fluid in the EDM stage changed the surface roughness (SR) properties. In this regard, the surface roughness values varied between 2.03 μm and 3.97 μm on average, depending on the discharge current, pulse duration and the change of different powder ratios added to the dielectric liquid.

Static contact angle measurements of HA, hBN and HA/hBN test samples at the same current intensity, discharge time and amount of nanopowder among the experimental design parameters are given in figure 5. Nanopowder concentrations affecting different processing conditions applied to the substrate material during the EDM stage cause different surface energies to occur on the surface. This depends on the amount of element by weight formed on the processed surface. However, in these measurements, it can be said that the residues formed on the surface, in other words the contaminations, exhibited hydrophobic properties in all samples with high surface energy. According to these measurements, the minimum contact angle obtained from the machined surface was obtained when HA was 15 g/l. In general, the maximum contact angle was determined in hBN-added processed test samples. This is due to the presence of the nitrogen (N) element in the hBN nanopowder element and its low affinity for water. For this reason, it has a more hydrophobic structure. Therefore, as the amount of nanopowder decreases, there is a serious decrease in surface energy. In addition, static contact angle measurements from all samples of HA/hBN nanopowder additives resulted similar. In these

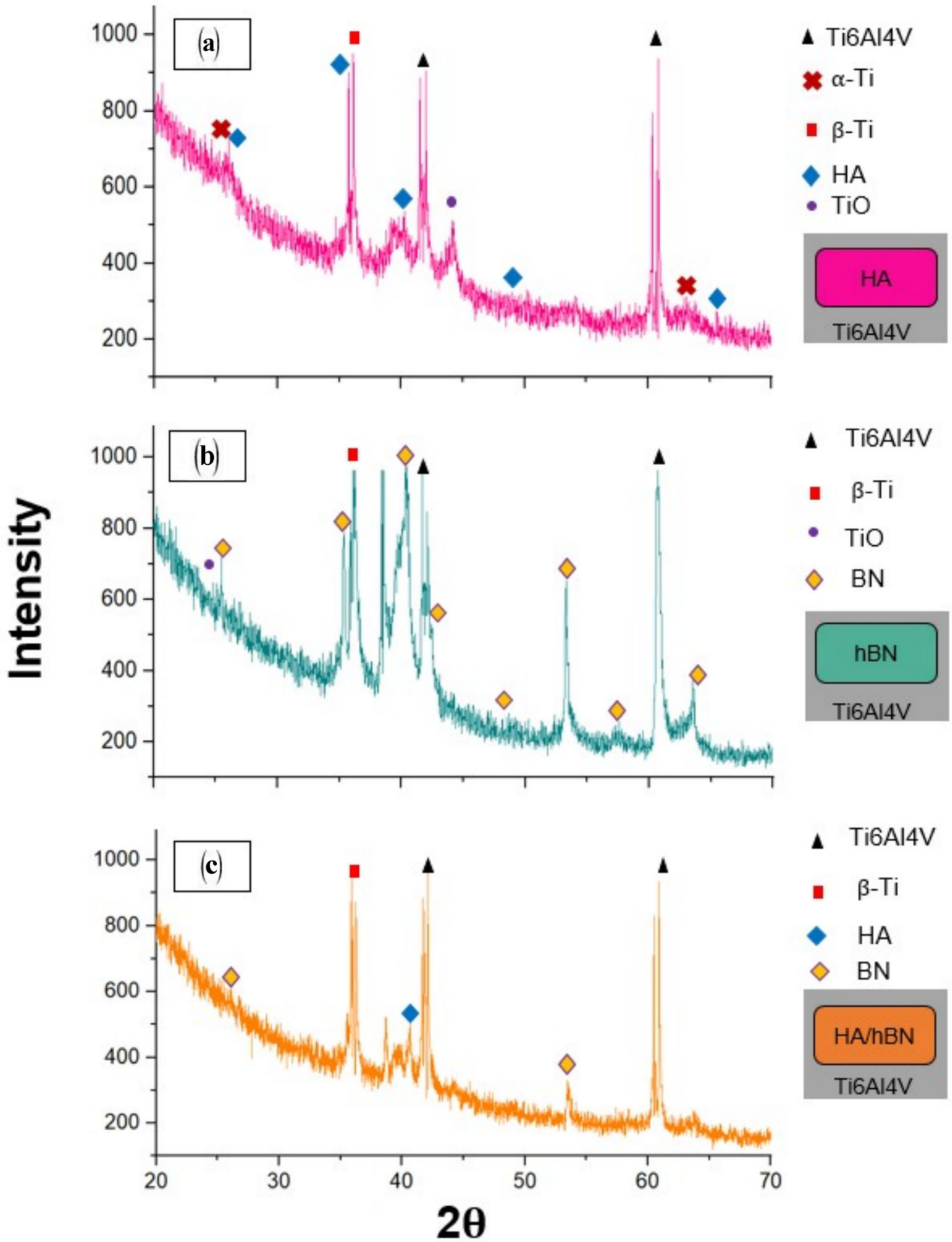
(a)
(b)
(c)
Intensity
2θ
1000
800
600
400
200
20
30
40
50
60
70
Ti6Al4V
α-Ti
β-Ti
HA
TiO
BN
HA
hBN
HA/hBN
Ti6Al4V

◀**Figure. 2.** X-ray diffraction (XRD) spectra of Ti6Al4V surfaces after PMEDM with (a) hydroxyapatite (HA), (b) hexagonal boron nitride (hBN), and c) HA/hBN powder additives in the dielectric liquid, showing the presence of new phases and successful incorporation of powders into the coating.

measurements, the forms of water droplets on the surface are always smooth.

3.2 *PMEDM machining factors optimization*

3.2.1 *ANOVA Analysis on the Impact of HA Powder Additive on MRR and SR* The ANOVA method is utilised to analyse experimental data and assess the impact of different parameters. It is a statistical tool that helps identify differences in the average performance of different groups of parts. ANOVA enables the determination of which parts are suitable for specific processes and their respective performance levels. The analysis of variance aims to assess the extent to which the elements being studied progress, the quality of the output values chosen for measurement, and the various levels that cause variations [44]. Table 3 indicates that none of the factors, including discharge current (I_p), pulse on time (t_{on}), and the combination of deionized water + hydroxyapatite, significantly influence the MRR, as evidenced by P values greater than 0.05. The discharge current, although having the highest percentage contribution of 32.75%, does not present a statistically significant effect at the conventional significance level. Similarly, pulse on time contributes 15.22% and the combination of deionized water + hydroxyapatite contributes 6.35%, neither of which is statistically significant. The residual error accounts for 45.66% of the total. Therefore, the statistical analysis suggests that the effects observed are not sufficient to conclude any dominant influence of these parameters under the current experimental conditions.

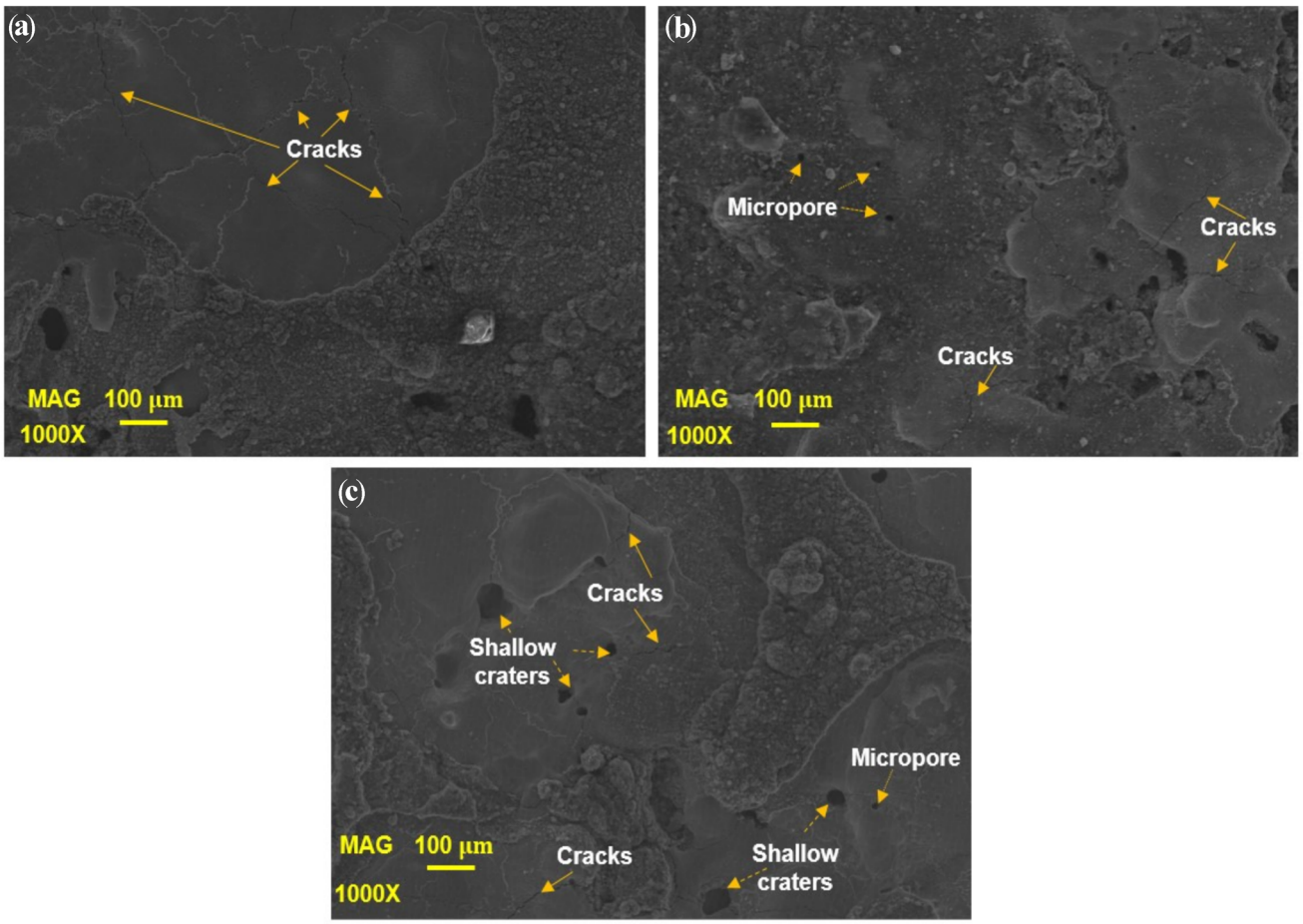

Figure. 3. SEM images of Ti6Al4V surfaces processed by PMEDM with additive powders: (**a**) hydroxyapatite (HA), (**b**) hexagonal boron nitride (hBN), and (**c**) HA/hBN mixture. Microstructural features such as micropores, microcracks, and craters generated by different process parameters and nanopowder additions are visible.

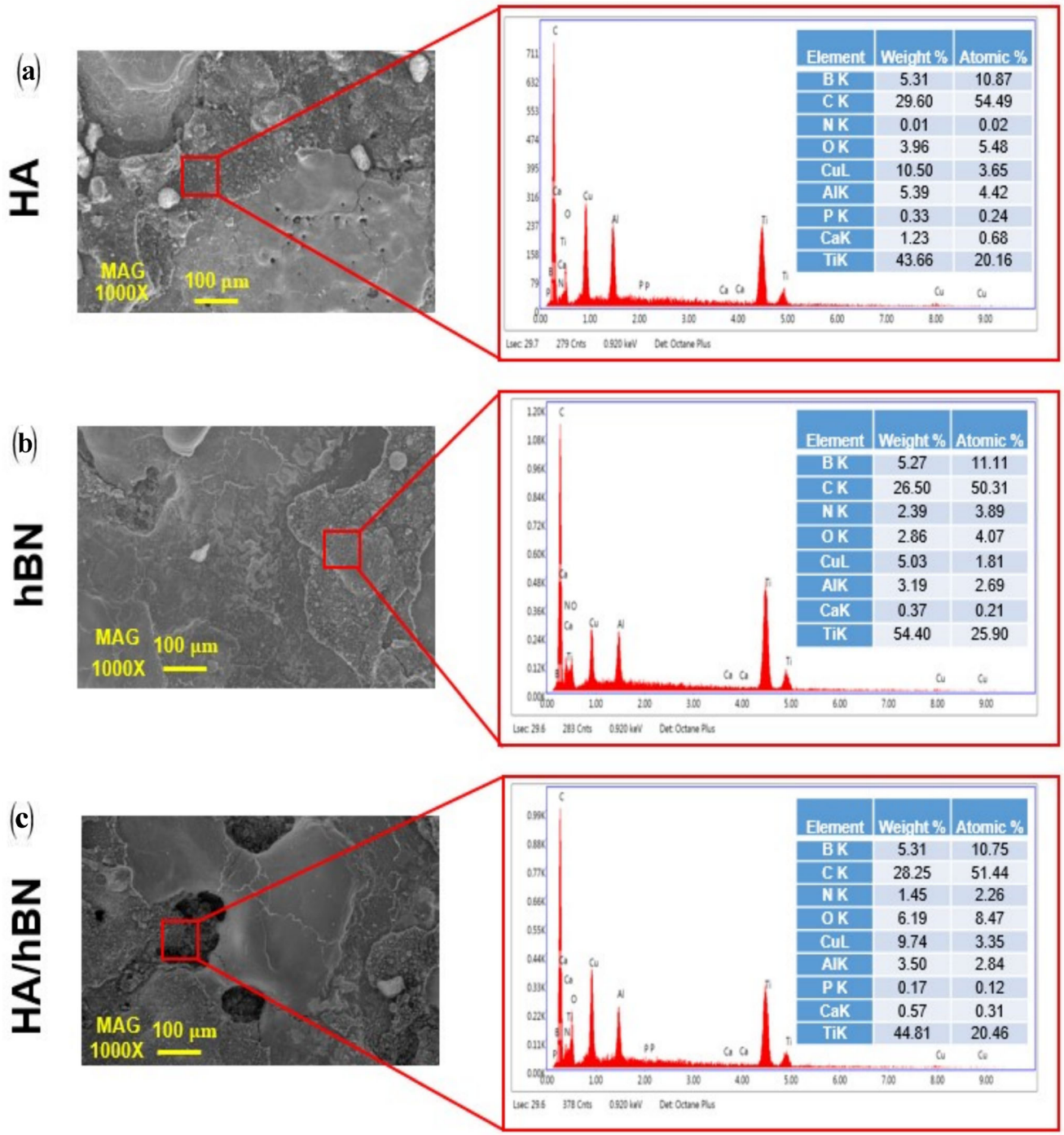

Figure. 4. Energy-dispersive spectroscopy (EDS) results for Ti6Al4V samples processed by PMEDM: (**a**) with HA, (**b**) with hBN, and **c** with HA/hBN powders. Detected element distributions confirm the presence and surface incorporation of the respective additives along with workpiece and electrode constituents.

Table 4 indicates that none of the factors, including discharge current (I_p), pulse on time (t_{on}), and the combination of deionized water + hydroxyapatite, significantly influence the surface roughness, as evidenced by P values greater than 0.05. The pulse on time accounts for the highest percentage contribution of 39.89% but does not exhibit a statistically significant effect at the conventional significance level. Discharge current and the combination of deionized water + hydroxyapatite contribute 9.42% and 5.88%, respectively, neither of which are statistically

Table 2. The surface roughness of PMEDM Ti6Al4V samples.

	#run		1	2	3	4	5	6	7	8	9
HA	Surface roughness (μ m)	SR #1	1.98	3.01	3.19	2.62	3.12	2.29	3.05	3.72	1.72
		SR #2	2.35	4.46	3.17	2.76	3.06	3.00	2.41	3.23	2.59
		SR #3	2.18	4.44	3.1	3.22	2.58	2.88	3.18	2.61	1.79
	Mean		2.17	3.97	3.15	2.86	2.92	2.72	2.88	3.18	2.03
	STDEV		0.18	0.83	0.55	0.83	0.31	0.48	0.04	0.29	0.41
hBN		SR #1	2.98	2.34	3.83	2.72	2.67	3.88	3.06	3.59	3.51
		SR #2	2.59	2.1	3.62	2.62	3.27	4.2	3.56	3.53	4.03
		SR #3	1.68	2.51	3.25	3.26	3.44	3.81	3.77	2.79	3.93
	Mean		2.41	2.32	3.56	2.86	3.12	3.96	3.46	3.30	3.82
	STDEV		0.66	0.21	0.44	0.21	0.34	0.27	0.29	0.40	0.36
HA/hBN		SR #1	2.52	3.07	2.73	2.32	2.75	2.94	2.97	2.25	2.6
		SR #2	2.2	4.24	2.9	2.45	2.2	2.95	2.75	2.36	2.92
		SR #3	2.84	4.66	2.08	2.73	2.81	2.7	2.82	2.05	2.65
	Mean		2.52	3.99	2.57	2.50	2.59	2.86	2.84	2.2	2.72
	STDEV		0.32	0.14	0.15	0.82	0.20	0.17	0.43	0.33	0.11

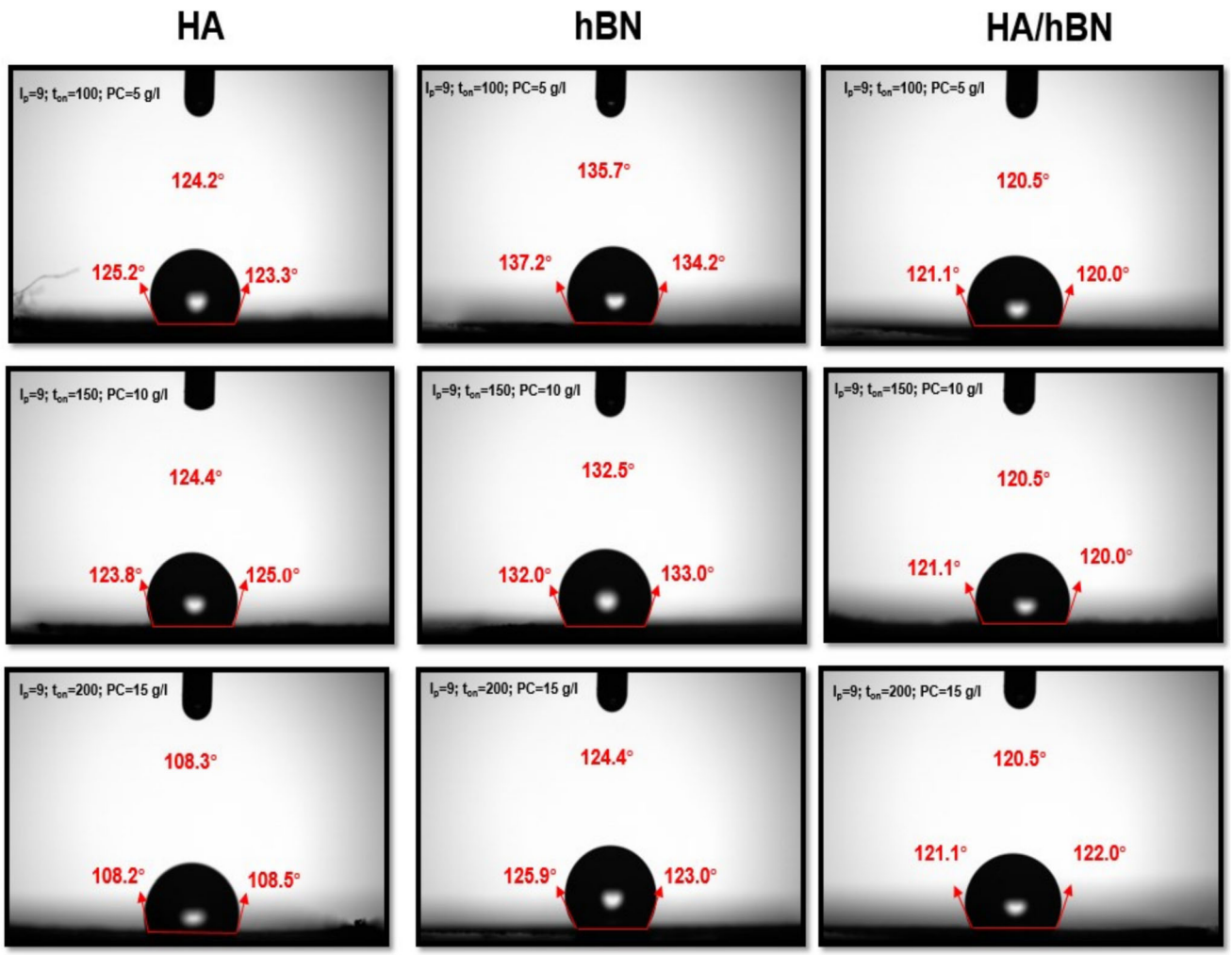

Figure. 5. Static water contact angle measurements for Ti6Al4V samples processed with PMEDM using HA, hBN, and HA/hBN powder additives at various concentrations, illustrating variations in surface wettability and hydrophobicity depending on powder type and process parameters.

Table 3. ANOVA Analysis Results for MRR

Source	DF	Adj SS	Adj MS	F-Value	*P*-Value	% Contribution
Discharge current, I_p (A)	2	0,000170	0,000085	0,72	0,582	32,7553
Pulse on time, t_{on} (µs)	2	0,000079	0,000040	0,34	0,749	15,22158
Deionized water+HA (g/l)	2	0,000033	0,000016	0,14	0,878	6,358382
Residual Error	2	0,000237	0,000118			45,66474
Total	8	0,000519				100

significant. The residual error accounts for 44.80% of the total. These results from the ANOVA analysis suggest that the observed effects of these parameters on surface roughness within the PMEDM processing context are not adequate to establish any significant influence under the current experimental conditions.

3.2.1.1. Taguchi analysis results for HA

It was observed, as illustrated in figure 6, that an increase in discharge current and pulse on time (t_{on}) correlates with an enhancement in MRR, whereas an increase in hydroxyapatite (HA) concentration leads to a reduction in MRR. This phenomenon can be attributed to the fact that elevated discharge current and t_{on} facilitate a quicker MRR. Conversely, an augmented HA concentration diminishes the frequency of discharge current within a specified timeframe, culminating in a decreased MRR. The impact of processing parameters on SR was similarly elucidated.

The interaction plot depicted in figure 7, examining the SR and MRR, reveals that there is a significant interaction among the process parameters, namely discharge current, pulse on time, and hydroxyapatite. This indicates that the outcomes of the electrical discharge machining process are significantly influenced by the interplay of these parameters. The interaction suggests that the optimization of the electrical discharge machining process to achieve desired SR and MRR necessitates a comprehensive understanding of how these parameters influence each other. Therefore, to enhance the efficiency and effectiveness of the machining process, it is imperative to consider the synergistic effects of discharge current, pulse on time, and hydroxyapatite concentration, as they collectively contribute to the machining performance.

Upon analysis of the MRR surface graph (figure 8), it is evident that an increment in current correlates with an enhancement in MRR. The MRR surface graph elucidates that as the discharge current increases; MRR also increases, while pulse duration has a negligible effect. Augmenting the peak current facilitates a greater energy density, thereby expediting the metal removal process. For all evaluated peak current parameters, an extension in pulse duration is associated with an increased MRR. Conversely, HA and pulse on time exhibit minimal influence on MRR. The efficiency of the process were gauged by the discharge current, determined by spark power and pulse rate per second. A regime of low discharge current coupled with high power culminates in an elevated rate of material removal. Notably, a reduction in pulse discharge current over time parallels enhancements in material cleanliness. A synergistic effect of prolonged pulse duration and elevated power were observed to yield a superior MRR. On the other hand, an investigation into the SR surface graph reveals that t_{on} and HA significantly affect surface roughness, more so than discharge current.

3.2.2 *ANOVA Analysis on the Impact of hBN Powder Additive on MRR and SR* In the study of PMEDM enhanced with hBN (hexagonal boron nitride) particle mixtures, the ANOVA results for MRR and SR are presented in Tables 5 and 6. The study on the PMEDM process, enhanced with hBN particles, reveals that the discharge current is the most significant factor affecting the MRR, contributing to 79.8% of its variance. It shows that higher discharge currents increase MRR by producing more energetic sparks, which melt and vaporize more material from the work piece. Conversely, pulse on time and the addition of hBN particles have minimal impact on MRR.

Table 4. ANOVA Analysis Results for SR

Source	DF	Adj SS	Adj MS	F-Value	*P*-Value	% Contribution
Discharge current, I_p (A)	2	0,2452	0,12261	0,21	0,826	9,424969
Pulse on time, t_{on} (µs)	2	1,0378	0,51888	0,89	0,529	39,89084
Deionized water+HA (g/l)	2	0,1531	0,07657	0,13	0,884	5,88484
Residual Error	2	1,1654	0,58271			44,79551
Total	8	2,6016				100

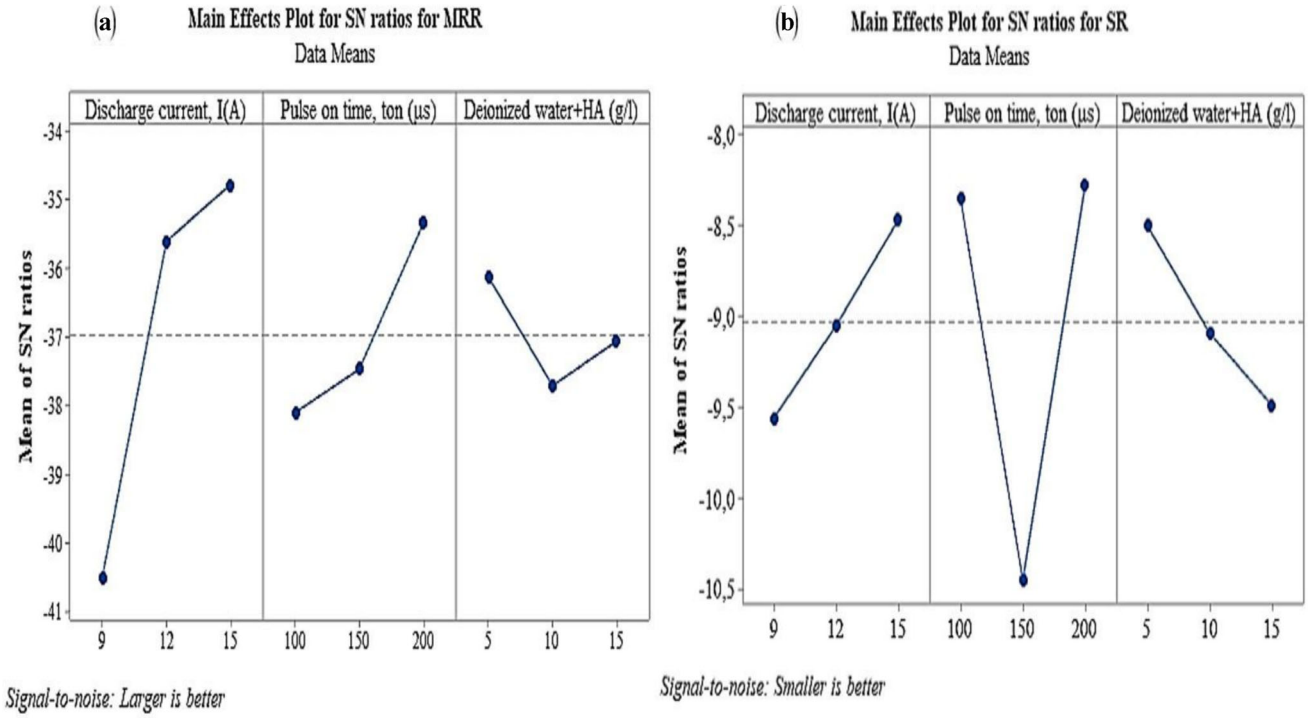

Figure. 6. Taguchi S/N ratio analysis for (**a**) material removal rate (MRR) and (**b**) surface roughness (SR) on PMEDM-processed Ti6Al4V using HA additive. Main effects of discharge current, pulse on time, and HA concentration are depicted.

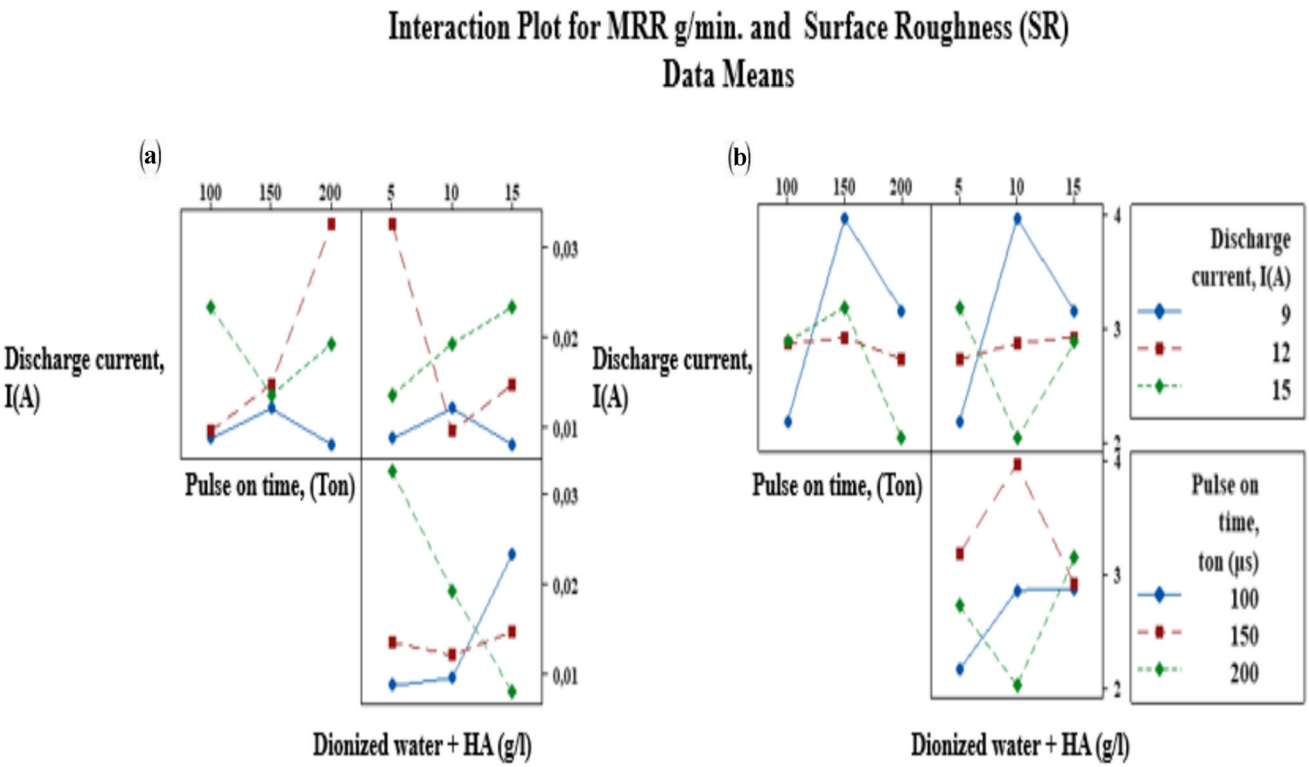

Figure. 7. Interaction plots showing the combined effects of discharge current, pulse on time, and HA concentration on (**a**) material removal rate (MRR) and (**b**) surface roughness (SR) for Ti6Al4V machined with HA-assisted PMEDM.

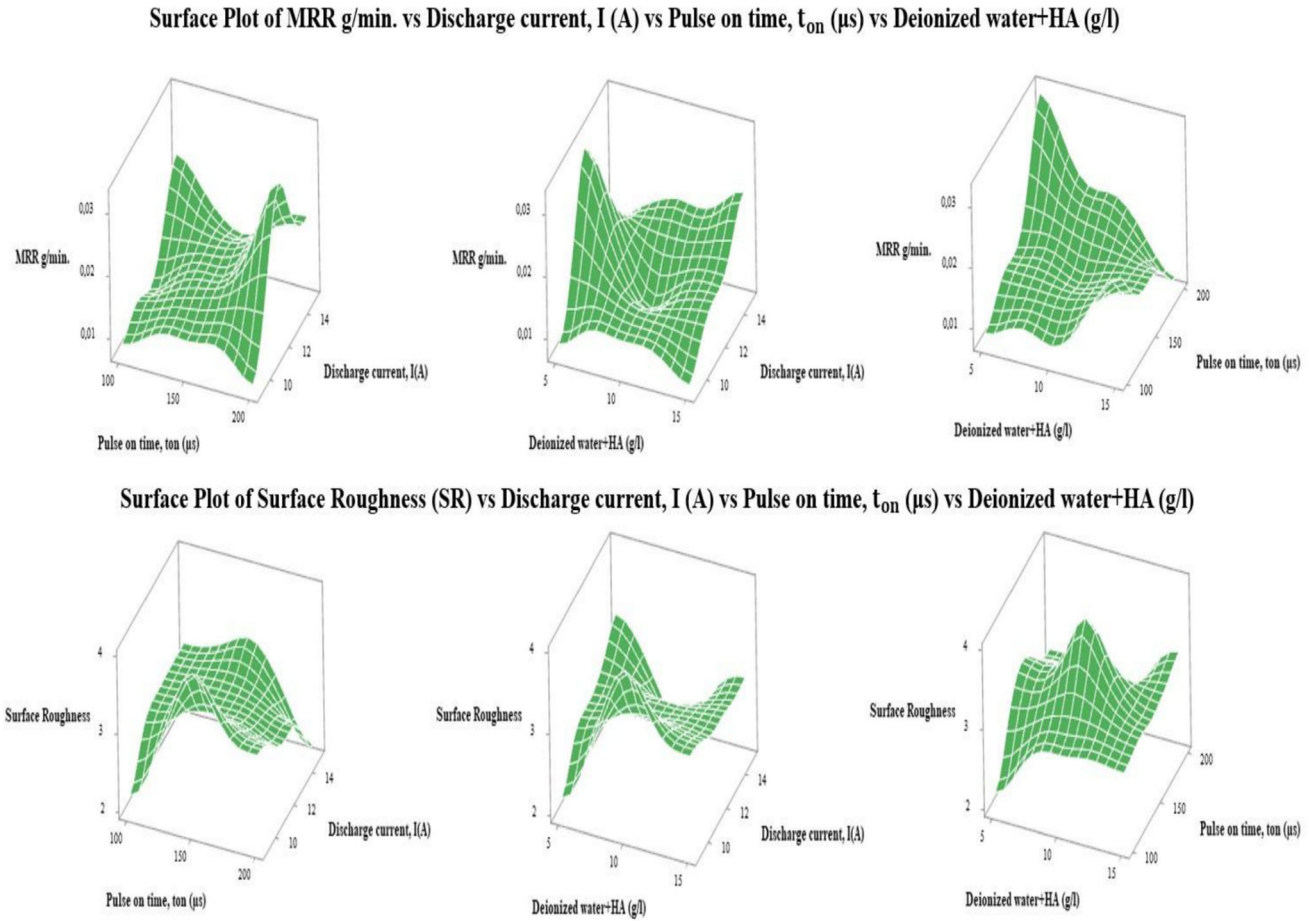

Figure. 8. Three-dimensional surface plots depicting the dependence of material removal rate (MRR) and surface roughness (SR) on discharge current, pulse on time, and HA concentration in the PMEDM process for Ti6Al4V.

However, both discharge current and pulse on time significantly influence surface roughness, with discharge current leading to a rougher surface due to more aggressive material removal. The addition of hBN particles does not significantly affect MRR or surface roughness but may offer other benefits like improved thermal properties of the dielectric fluid or reduced electrode wear, which were not the focus of this study. This aligns with the understanding that energy input is crucial for material removal efficiency in PMEDM, while the impact of process additives and timing parameters on outcomes like MRR and surface roughness may be less direct.

3.2.2.1. Taguchi analysis results for hBN

Figure 9 is drawn according to the results obtained in the experiments. In the investigation of PMEDM enhanced with the addition of hBN particles, the Taguchi method results for MRR and SR indicate that an increase in input parameters (discharge current, pulse on time, and hBN concentration) leads to improvements in both MRR and surface quality. This phenomenon can be elucidated by considering the underlying mechanisms of PMEDM processing and the role of hBN particles.

This study investigates the effects of discharge current, pulse on time, and hBN particle concentration on the

Table 5. ANOVA Analysis Results for MRR

Source	DF	Adj SS	Adj MS	F-Value	*P*-Value	% Contribution
Discharge current, I_p (A)	2	0,000333	0,000166	41,34	0,024	79,85612
Pulse on time, t_{on} (µs)	2	0,000007	0,000003	0,85	0,540	1,678657
Deionized water+ hBN (g/l)	2	0,000069	0,000035	8,58	0,104	16,54676
Error	2	0,000008	0,000004			1,918465
Total	8	0,000417				100

Table 6. ANOVA Analysis Results for SR

Source	DF	Adj SS	Adj MS	F-Value	*P*-Value	% Contribution
Discharge current, I_p (A)	2	0,92945	0,46472	29,64	0,033	34,50087
Pulse on time, t_{on} (μs)	2	1,51148	0,75574	48,20	0,020	56,10563
Deionized water+ hBN (g/l)	2	0,22169	0,11085	7,07	0,124	8,229058
Error	2	0,03136	0,01568			1,164073
Total	8	2,69399				100

PMEDM process. The main findings indicate a significant increase in MRR and surface quality with higher parameter values. Increasing discharge current enhances MRR by facilitating more effective melting and vaporization of the workpiece material, while longer pulse on times contribute to increased MRR by enabling prolonged energy delivery. The hBN particles may assist in the material removal process by potentially improving the distribution of spark energy due to their thermal and electrical properties. Contrary to the expectation that higher discharge energies would negatively impact surface quality, the study observes an improvement in surface quality with increased input parameters. The hBN particles could contribute to achieving a finer surface finish by promoting a more uniform distribution of sparks and more evenly distributed craters on the workpiece surface. Additionally, the presence of hBN particles may aid in enhancing the removal of debris from the machining zone, thereby reducing surface irregularities. The research highlights the complexity of the PMEDM process and emphasizes the need for a comprehensive understanding of how the interaction between discharge current, pulse on time, and hBN concentration collectively influences machining outcomes. The presence of hBN particles introduces a significant variable that can alter the dynamics of the PMEDM process, affecting both material removal efficiency and surface quality. The findings from the Taguchi method analysis suggest that careful management of these parameters, particularly considering the role of process additives like hBN particles, can optimize both productivity and surface integrity in hBN-augmented PMEDM processes. This underscores the potential for process additives to significantly modify the characteristics of PMEDM machining, offering new avenues for optimising both material removal efficiency and the quality of the machined surface.

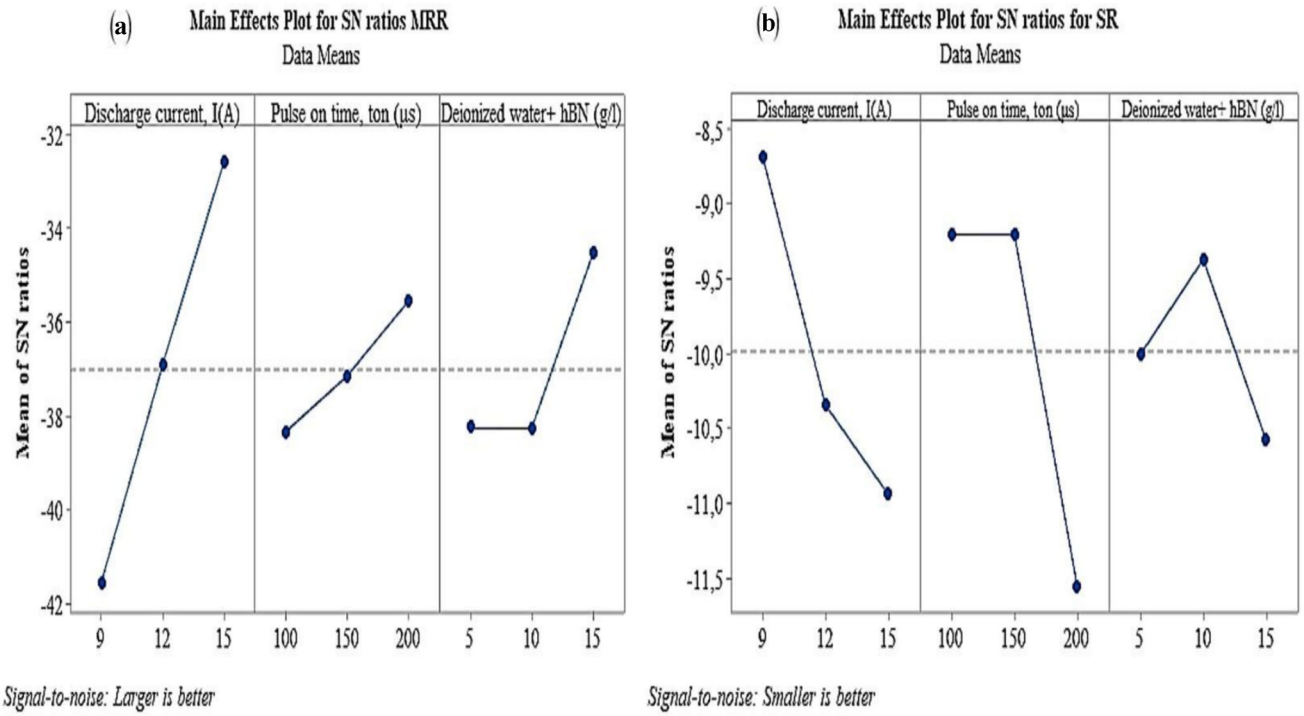

Figure. 9. Signal-to-noise (S/N) ratio main effects plots for (**a**) MRR and (**b**) SR, presenting the influence of discharge current, pulse duration, and hBN concentration in PMEDM of Ti6Al4V.

In the study of PMEDM augmented with hBN particles, the interaction plots (figure 10) for MRR and SR reveal that the input parameters (discharge current, pulse on time, and the addition of hBN particles) are in interaction with one another. This indicates that the effects of these parameters on MRR and SR are not independent but rather interdependent, influencing the machining outcomes in a complex manner. This observation underscores the necessity of considering the combined effects of these parameters when optimising the PMEDM process for enhanced performance and surface quality.

When examining the surface plot in figure 11, it is observed that an increase in discharge current correlates with an increase in MRR. However, the addition of hBN particles and pulse on time appear to have a negligible impact on MRR. This suggests that the contribution of hBN particles to MRR is minimal. On the other hand, when analysing surface roughness, both discharge current and the presence of hBN particles significantly influence the outcome. An increase in these parameters is associated with an increase in surface roughness values. This interpretation is derived from the results of machining by the PMEDM process.

3.2.3 *ANOVA analysis on the impact of HA/hBN powder additive on MRR and SR* In the PMEDM process using HA/hBN particle mixtures, ANOVA results showed that discharge current had the greatest influence on material removal rate (MRR), accounting for 37.3% of the variance. Although P-values were above 0.05, this parameter still played a key role: higher currents led to more energetic sparks and improved material removal. The HA/hBN mixture also contributed 10.2% to MRR changes, possibly by improving conductivity and spark efficiency. For surface roughness (SR), discharge current, pulse duration, and HA/hBN mixture influenced the results, with the mixture contributing to smoother finishes by altering spark and cooling behavior. Overall, adding particle mixtures like HA/hBN affects both efficiency and quality in PMEDM.

It is noteworthy that the ANOVA analyses across all powder additives (Tables 3, 4, 5, 6, 7 and 8) exhibit relatively high residual error percentages (ranging from 44-50% for several analyses). These elevated residual values warrant further discussion as they represent unexplained variability in the experimental outcomes. Several factors may contribute to this observation:

First, the PMEDM process involves complex multiphysics phenomena including thermal, electrical, and material interactions that may not be fully captured by the three parameters investigated in this study. Second, there may exist non-linear interactions between parameters that our experimental design did not explicitly address. Third, the inherently stochastic nature of spark generation in EDM introduces natural variability in the process outcomes. Fourth, the microscale nature of material modifications introduces challenges in measurement precision that may contribute to observed variability. Despite these limitations, the relative contributions of the parameters identified remain valuable for understanding their hierarchical

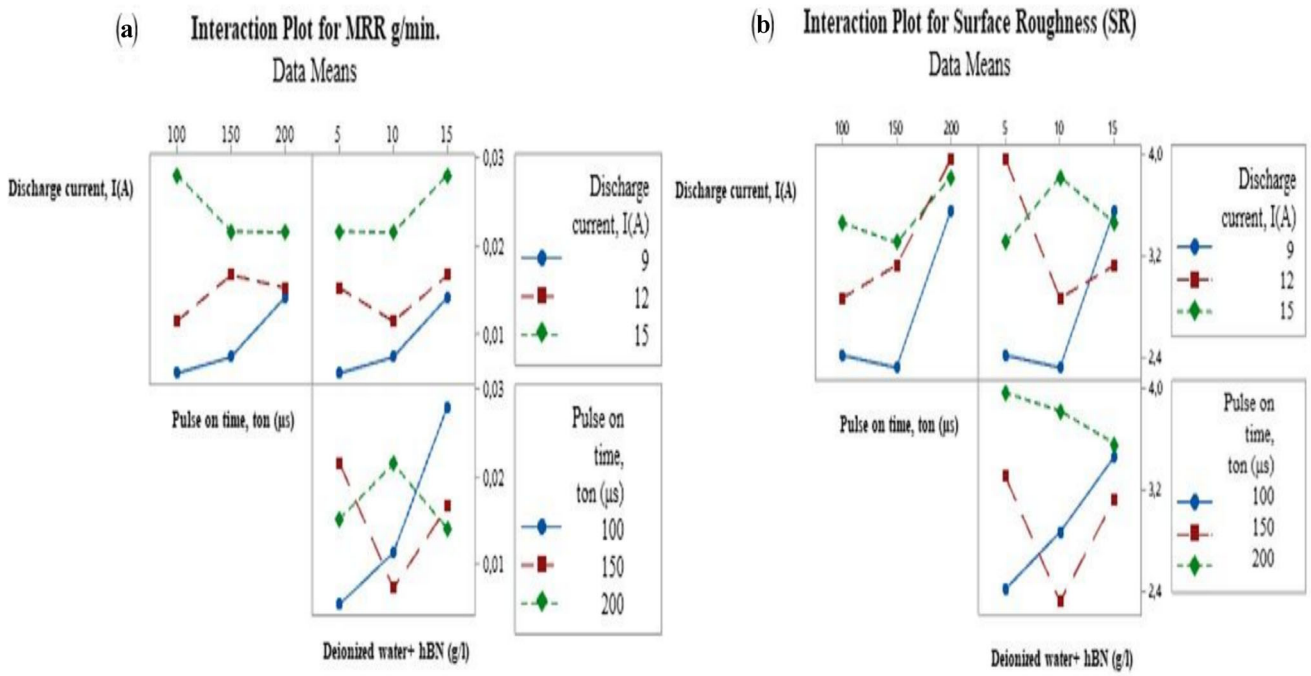

Figure. 10. Interaction plots illustrating how discharge current, pulse on time, and hBN concentration jointly affect (**a**) material removal rate (MRR) and (**b**) surface roughness (SR) in PMEDM processing with hBN powders.

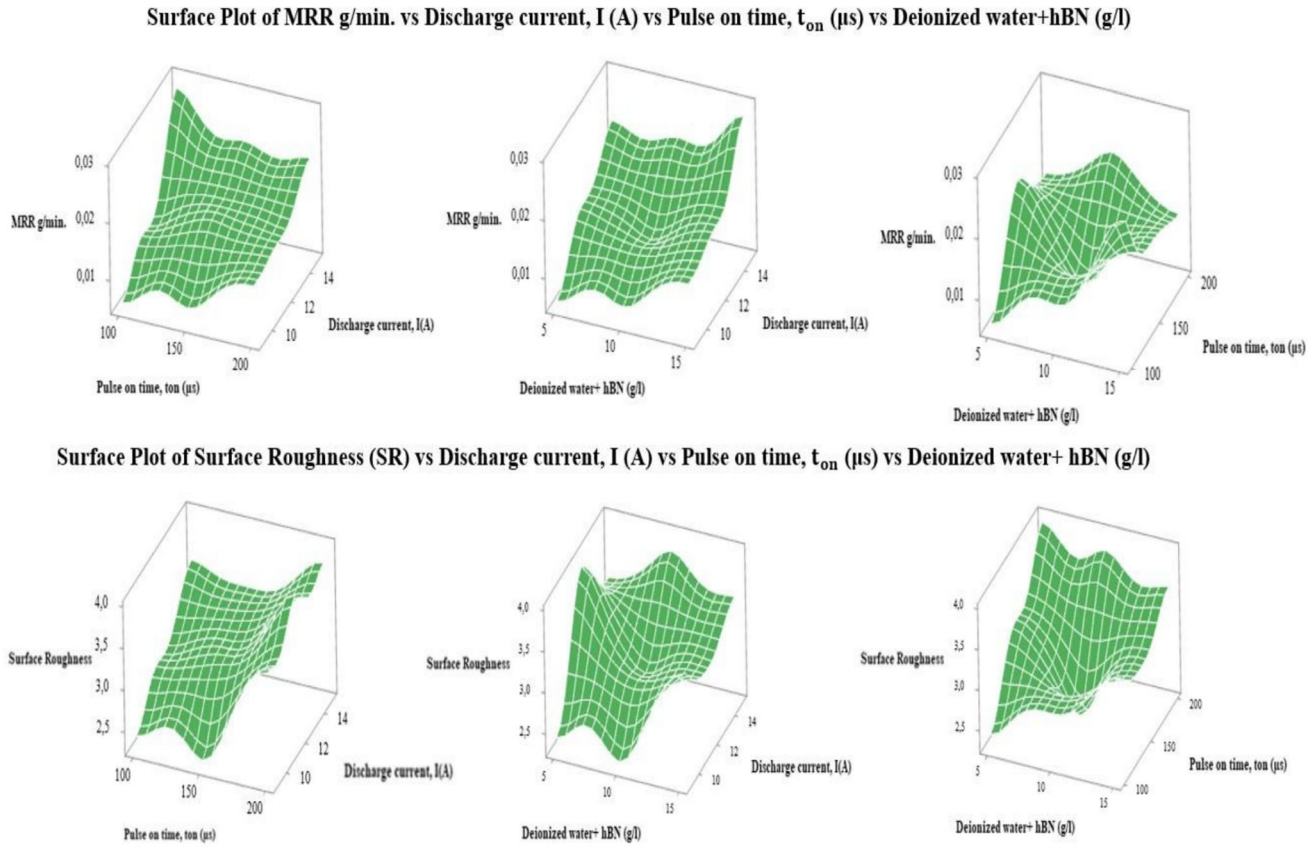

Figure. 11. 3D surface plots showing material removal rate (MRR) and surface roughness (SR) as functions of discharge current, pulse on time, and hBN concentration in PMEDM of Ti6Al4V alloy.

Table 7. ANOVA Analysis Results for MRR

Source	DF	Adj SS	Adj MS	F-Value	*P*-Value	% Contribution
Discharge current, I_p (A)	2	0,000044	0,000022	0,78	0,562	37,28814
Pulse on time, t_{on} (µs)	2	0,000005	0,000003	0,09	0,919	4,237288
Deionized water+ HA/hBN (g/l)	2	0,000012	0,000006	0,21	0,828	10,16949
Error	2	0,000057	0,000028			48,30508
Total	8	0,000118				100

Table 8. ANOVA Analysis Results for SR

Source	DF	Adj SS	Adj MS	F-Value	*P*-Value	% Contribution
Discharge current, I_p (A)	2	0,2530	0,1265	0,28	0,779	14,27201
Pulse on time, t_{on} (µs)	2	0,2756	0,1378	0,31	0,763	15,54691
Deionized water+ HA/hBN (g/l)	2	0,3545	0,1772	0,40	0,715	19,99774
Error	2	0,8896	0,4448			50,18334
Total	8	1,7727				100

importance in the PMEDM process. Future work could employ more sophisticated experimental designs such as Taguchi method or incorporate additional parameters such as gap voltage, duty cycle, or dielectric flushing pressure to potentially account for more of the observed variability. Additionally, increasing the number of experimental

repetitions could help reduce random variability and provide more robust statistical insights.

3.2.3.1. Taguchi analysis results for HA/hBN

Upon examining the results of the Taguchi analysis provided, it is observed that an increase in current leads to an increase in MRR. Additionally, an increase in the input parameters has also resulted in an increase in SR. These outcomes from the PMEDM process can be interpreted and explained as follows:

When figure 12 are examined, the relationship between increased current and higher MRR can be attributed to the fundamental principle that the discharge current directly influences the energy of the sparks generated between the electrode and the workpiece. A higher current translates to more energetic sparks, which in turn have the capacity to melt and vaporize a larger volume of material from the workpiece. This increased energy input into the machining zone facilitates a more efficient material removal process, thereby elevating the MRR. The direct correlation between current intensity and spark energy forms the basis for this observed outcome. The observation that an increase in the input parameters leads to an increase in surface roughness can be explained by considering the nature of the PMEDM process. Higher current and longer pulse durations, which are among the input parameters, result in larger and deeper craters on the workpiece surface due to the more intense and prolonged energy discharge. While these conditions are conducive to higher MRR, they also tend to produce a rougher surface texture, as the larger craters and the irregularities between them contribute to increased surface roughness. Additionally, other input parameters that enhance the energy input into the machining zone can similarly exacerbate the formation of surface defects, leading to a deterioration in surface finish.

In summary, the findings from the Taguchi analysis highlight the inherent trade-offs between maximising MRR and minimising SR in the PMEDM process. The increase in current and other input parameters enhances the efficiency of material removal at the cost of surface finish quality. This underscores the importance of carefully balancing the input parameters in PMEDM to achieve the desired outcomes, taking into account the specific requirements of the machining operation in terms of both productivity and surface integrity.

The analysis of the interaction plot in PMEDM processing reveals that the input parameters (discharge current, pulse on time, and hBN concentration) significantly interact with each other, influencing both MRR and SR (figure 13). The interaction between discharge current and pulse on time fundamentally affects the energy delivered to the workpiece, with their combined effect on energy delivery being multiplicative rather than additive. This interaction can increase MRR but might also worsen surface finishes due to larger crater formation.

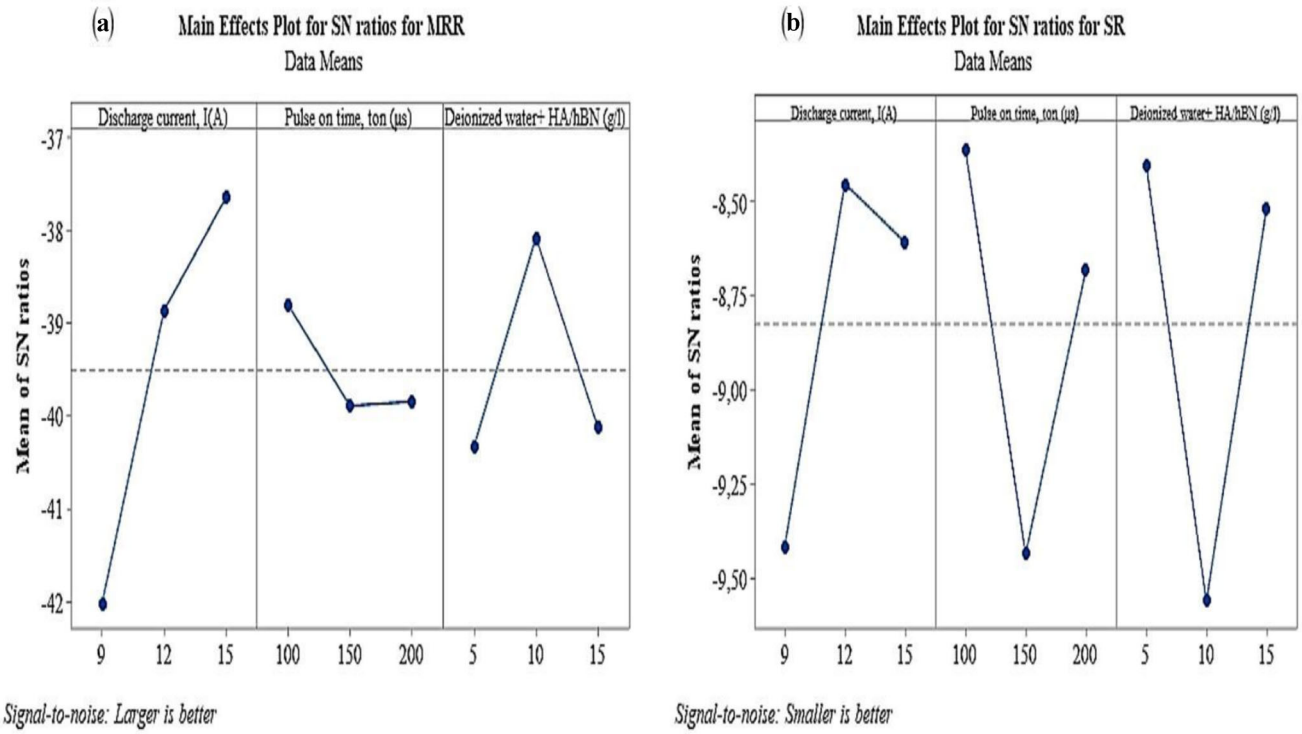

Figure. 12. Main effects plots (signal-to-noise ratio) for (**a**) MRR and (**b**) SR, demonstrating the contribution of discharge current, pulse duration, and HA/hBN concentration in PMEDM of Ti6Al4V alloy.

The introduction of hBN particles to the dielectric fluid adds a third dimension to this interaction, altering the fluid's electrical conductivity and thermal properties, thus affecting spark efficiency and characteristics. This can modify MRR and SR, depending on how the hBN concentration influences energy distribution and debris removal during machining. The interactions among all three parameters highlight the complexity of PMEDM, showing both synergistic and antagonistic effects depending on parameter combinations. This underscores the need for a holistic approach to PMEDM process optimization, considering all parameters' combined effects to achieve the desired balance between MRR and SR.

The examination of figure 14 reveals distinct trends regarding the effects of discharge current, pulse on time, and HA/hBN concentration on MRR and SR in PMEDM processing. The increase in MRR with higher discharge currents is attributed to the generation of more energetic sparks, capable of melting and vaporizing material from the workpiece more effectively. Conversely, the decrease in MRR with longer pulse on times and higher HA/hBN concentrations can be explained by the more widespread energy distribution and potential alterations in the dielectric fluid's properties due to the presence of hBN particles, which may reduce spark generation or energy transfer efficiency. The increase in SR with higher discharge currents, longer pulse on times, and greater HA/hBN concentrations can be linked to the formation of larger and deeper craters on the workpiece surface and the potential complexity introduced by HA/hBN particles in the surface texture. This may lead to uneven surface formations and consequently higher SR. In conclusion, the interactions among discharge current, pulse on time, and HA/hBN concentration impact material removal efficiency and surface quality in PMEDM processing. These observations underscore the importance of a comprehensive understanding of parameter interactions for optimising PMEDM processes and highlight the need to strike a balance between efficiency and surface integrity to achieve the desired machining outcomes.

The synergistic incorporation of HA and hBN nanopowders in the PMEDM process yields composite surfaces on Ti6Al4V alloys that exhibit significantly enhanced functional properties compared to those achieved with either additive alone. SEM and EDS analyses confirm that the HA/hBN combination generates a more homogeneous and refined microstructure, characterized by evenly distributed micropores, microcracks, and shallow craters. This microstructural regularity not only optimizes surface roughness and mechanical integrity but also supports favorable biological interactions.

Mechanistically, the inclusion of hBN nanosheets within the HA matrix acts as a reinforcing phase, restricting crack propagation and fostering a denser coating morphology.

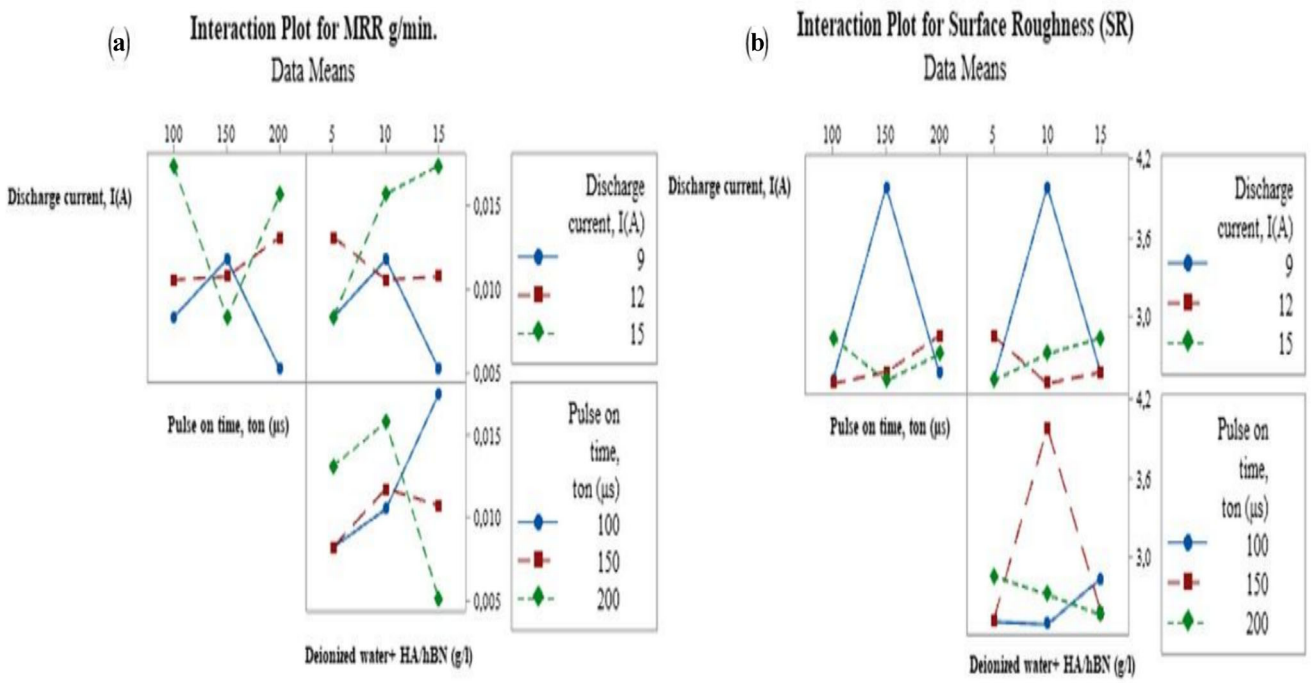

Figure. 13. Interaction plots displaying the combined effects of discharge current, pulse on time, and HA/hBN concentration on (**a**) material removal rate (MRR) and (**b**) surface roughness (SR) for Ti6Al4V processed by PMEDM with a mixture of HA and hBN powders.

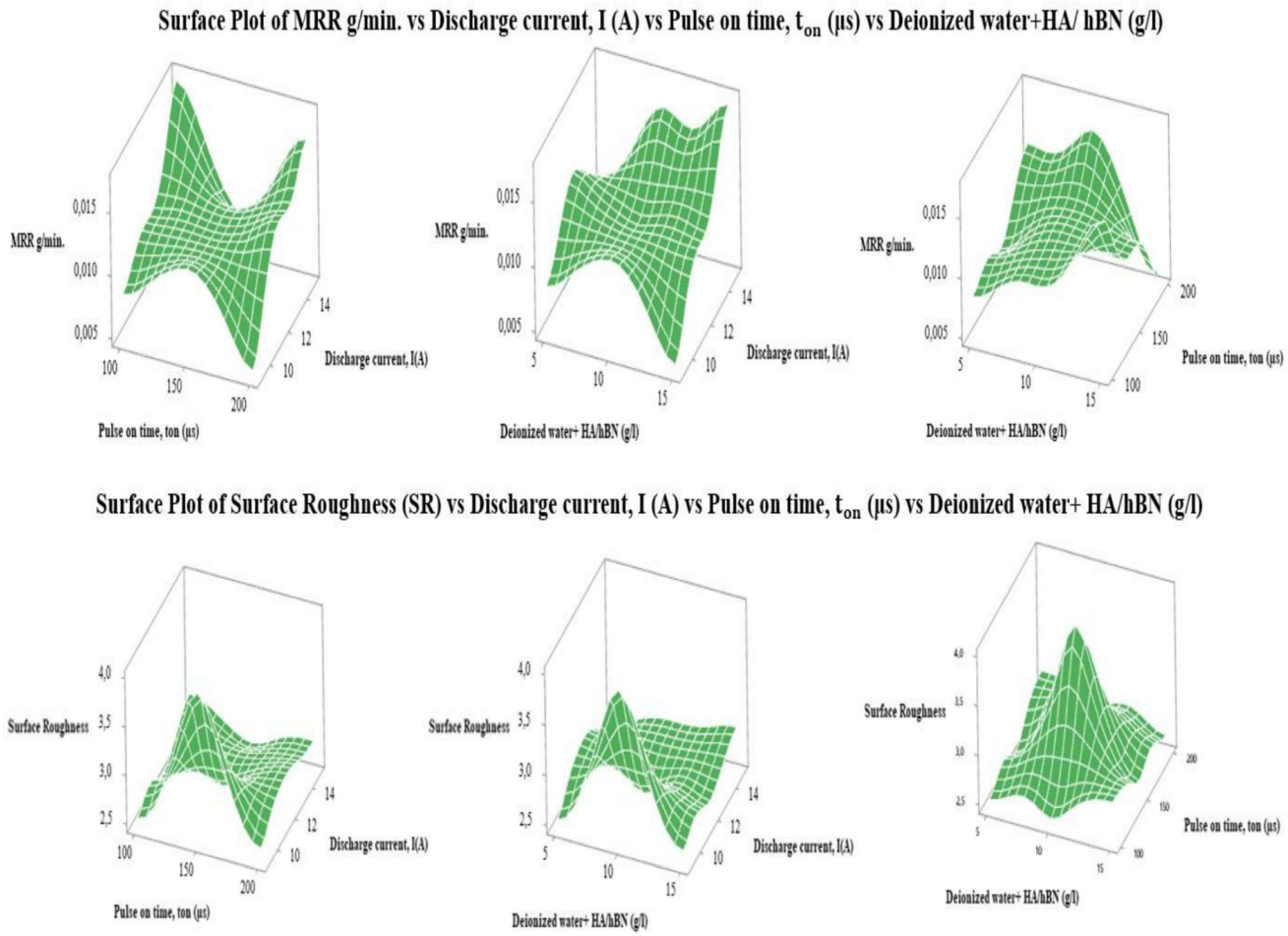

Figure 14.. Three-dimensional surface plots illustrating the relationship of MRR and SR to discharge current, pulse on time, and HA/hBN powder concentration for PMEDM-processed Ti6Al4V samples.

HA, meanwhile, supplies bioactive sites essential for cellular attachment and proliferation. The interaction between these two phases gives rise to a surface environment that simultaneously supports cell adhesion and suppresses bacterial colonization. This are evidenced by contact angle measurements and biofilm analyses, which indicate that HA/hBN-modified surfaces exhibit optimal hydrophilicity, as well as reduced bacterial attachment compared to single-phase coatings. Moreover, hBN's well-documented bacteriostatic and bactericidal properties, likely arising from oxidative stress induction and membrane disruption, complement the biocompatibility and osteoconductivity of HA. The coexistence of both components may also fine-tune the local charge distribution and surface energy, further affecting protein adsorption, cell behavior, and resistance to bacterial adhesion.

In summary, the superior performance observed in HA/hBN composite coatings derives from the interplay of multiple mechanisms: structural reinforcement by hBN, enhanced bioactivity provided by HA, beneficial modulation of surface properties such as wettability and roughness, and the antibacterial influence primarily afforded by hBN. This synergy enables the engineering of multifunctional surface coatings with both robust mechanical performance and advanced biofunctionality, making HA/hBN composites especially promising for demanding biomedical implant applications. The comparative approach adopted in this study provides insights into the effects of HA, hBN, and their combination on both mechanical and biological responses of Ti6Al4V alloys, contributing to existing knowledge by offering systematic data under consistent experimental conditions.

3.3 *Bioactivity of the PMEDM treated surface*

In statistical comparison of the test samples, 2h, 4h and 6h incubation samples were compared separately. For the 2h incubation period, all test samples were found to be forming higher BCR compared to untreated control, but there were no significant differences between them (F = 14.176, df = 3, p<0.05). For 4h and 6h incubation period, all test samples had the same BCR in comparison to untreated

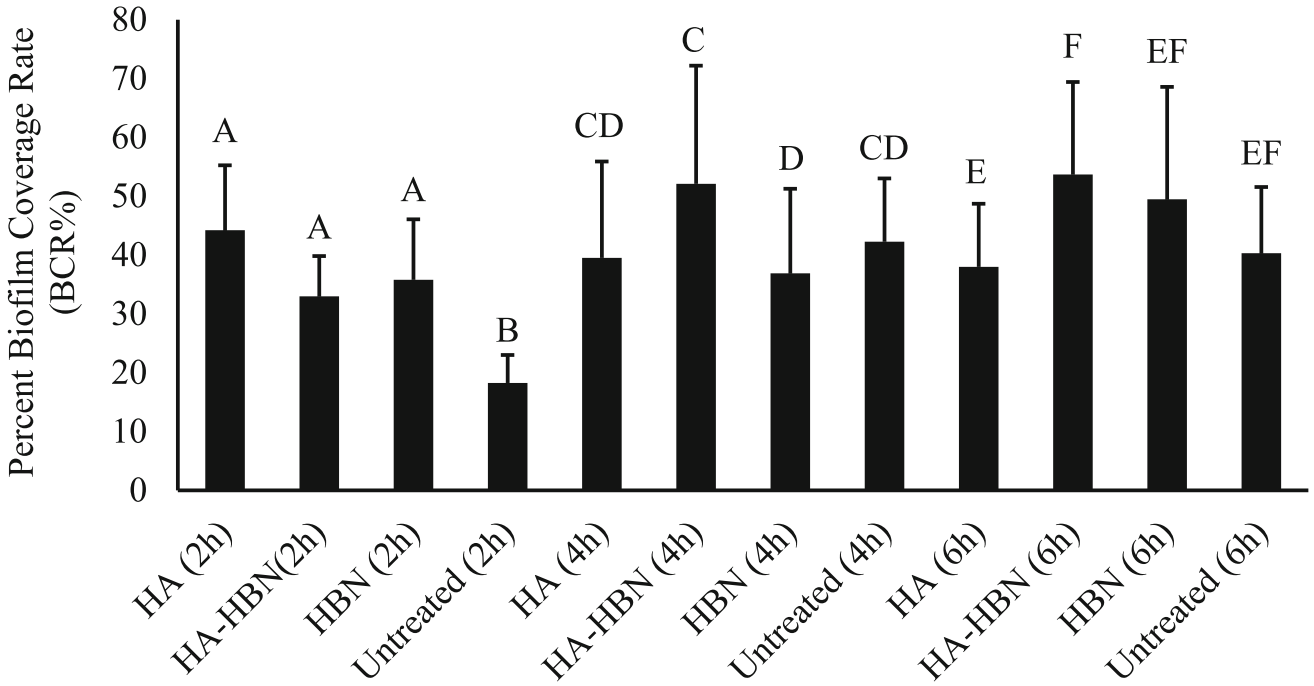

Figure 15.. Percent biofilm coverage rate (BRC) of test samples and untreated control. HA; Hydroxyapatite, HA/HBN; Hydroxyapatite-Hexagonal boron nitride, HBN; Hexagonal boron nitride, Untreated; Ti6Al4V. 2h, 4h and 6h; 2 hours, 4 hours, and 6 hours, respectively. The same capital letters indicate no significant difference between treatments (2h, 4h and 6h were evaluated separately) according to LSD multiple comparison test ($p<0.05$).

control ($F = 1.605$, $df = 3$, $p>0.05$ for 4h and $F = 2.331$, $df = 3$, p>0.05) (figure 15). In figure 15, the biofilm coverage rate (BCR) for HA decreases while all other combinations show an increasing trend. This observation can be justified by considering the specific interactions between the HA particles and the bacterial cells. Hydroxyapatite (HA) is known for its biocompatibility and osteoconductive properties, which can promote cell attachment and proliferation. However, in the context of biofilm formation, the HA particles might have created a surface environment that is less conducive to biofilm development over time. This could be due to the release of calcium and phosphate ions from the HA, which might inhibit bacterial adhesion or disrupt the biofilm matrix. In contrast, the other combinations, including HA/hBN and hBN, might have provided a more stable surface for biofilm formation, leading to an increasing trend in BCR.

Figure 16 presents microscopic images of the test samples alongside the untreated control, illustrating bacterial biofilm formation at various incubation intervals (2 hours, 4 hours, and 6 hours). The images elucidate the following observations regarding the formed elements and their compositions:

HA (Hydroxyapatite): The images show a decrease in biofilm coverage over time, which could be attributed to the inhibitory effects of calcium and phosphate ions released from the HA particles. These ions might interfere with bacterial adhesion and biofilm matrix stability.

- HA/hBN (Hydroxyapatite-Hexagonal Boron Nitride): The images indicate a relatively stable biofilm coverage, suggesting that the combination of HA and hBN particles provides a balanced environment for biofilm formation. The hBN particles might enhance the mechanical stability of the biofilm, while the HA particles contribute to biocompatibility.
- hBN (Hexagonal Boron Nitride): The images show an increasing trend in biofilm coverage, indicating that hBN particles alone provide a favorable surface for biofilm development. The thermal and electrical properties of hBN might contribute to a more uniform distribution of bacterial cells and biofilm matrix.
- Untreated (Ti6Al4V): The images show a consistent increase in biofilm coverage over time, which is expected for the untreated control. The Ti6Al4V alloy provides a standard surface for bacterial adhesion and biofilm formation without any additional effects from particle additives.

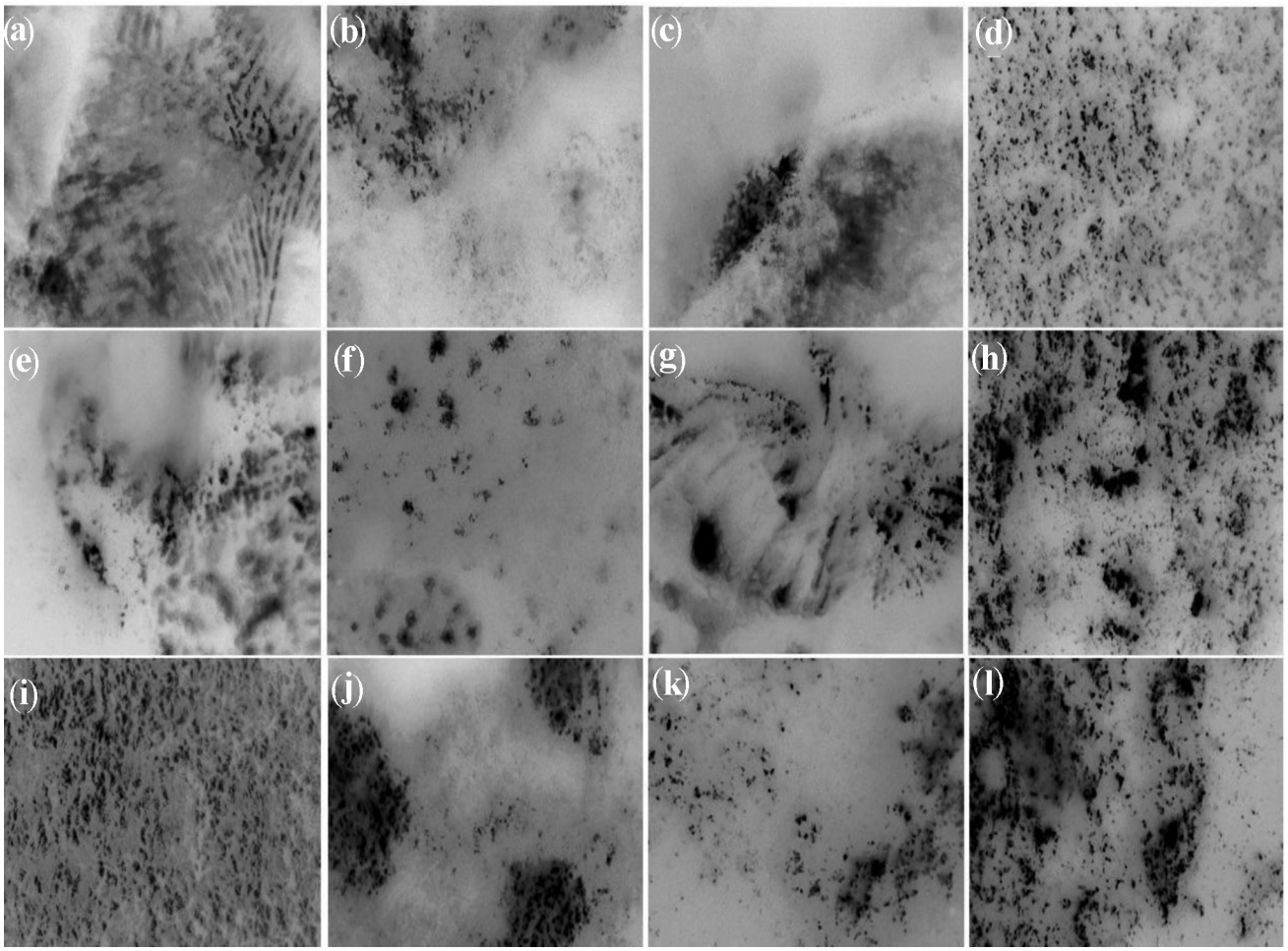

Figure 16.. Microscopic images of the test samples and untreated control showing bacterial biofilm formation. A, B, C and D; 2h samples and HA (hydroxyapatite), HA/hBN (hydroxyapatite-hexagonal boron nitride), hBN (hexagonal boron nitride) and Untreated (Ti6Al4V), respectively. E, F, G and H; 4h samples and HA (hydroxyapatite), HA/hBN (hydroxyapatite-hexagonal boron nitride), hBN (hexagonal boron nitride) and Untreated (Ti6Al4V), respectively. I, J, K and L; 6h samples and HA (hydroxyapatite), HA/hBN (hydroxyapatite-hexagonal boron nitride), hBN (hexagonal boron nitride) and Untreated (Ti6Al4V), respectively.

4. Conclusions

Our findings underscore the paramount influence of discharge current on MRR, attributing its primary role to the enhanced energy of sparks between the electrode and workpiece, facilitating more efficient material melting and vaporization. Concurrently, pulse on time and the incorporation of HA/hBN particles emerge as critical factors in modulating SR, revealing the intricate dynamics of their interaction with discharge current in determining the overall machining outcomes.

The strategic addition of HA/hBN particles to the PMEDM process introduces nuanced variables that significantly impact both the efficiency and quality of machining. While elevated discharge currents and extended pulse durations are generally conducive to increased MRR, they potentially compromise surface quality by engendering larger and more profound craters. In contrast, the presence of HA/hBN particles appears to mitigate these adverse effects, ostensibly leading to enhanced surface finishes through a more uniform distribution of sparks and facilitation of debris removal, without markedly influencing MRR.

This investigation brings to light the inherent trade-offs between optimizing MRR and minimizing SR, accentuating the imperative for a holistic comprehension of the interplay among process parameters to refine the machining process. Our results advocate for a judicious approach to parameter selection, aimed at concurrently elevating material removal efficiency and surface integrity, to achieve the requisite machining performance. This research enriches the corpus of knowledge in EDM,

illustrating the transformative potential of process additives like HA/hBN particles in significantly altering machining characteristics and paving new pathways for the optimization of PMEDM processes.

Furthermore, through a controlled experimental study, we meticulously examined the impact of powder additive concentration on biofilm formation over durations of 2, 4, and 6 hours, employing materials enhanced with 5 g, 10 g, and 15 g of powder additives. The study delineates a nuanced understanding of biofilm dynamics, highlighting that the concentration of powder additives and the duration of exposure profoundly influence biofilm formation on material surfaces. Initial observations indicated a promotion of biofilm growth in the short term with a 5 g powder additive, while a 10 g concentration exhibited a biofilm inhibitory effect, except in the case of the HA/hBN particles, which suggested a synergistic enhancement of biofilm growth. Extending the exposure to a 15 g powder additive further corroborated the promotion of biofilm formation, underlining the complexity of biofilm dynamics and the potential for customizing surface treatments to either foster or hinder biofilm growth, contingent upon the desired outcomes.

While our ANOVA analyses revealed considerable unexplained variability (as evidenced by high residual error percentages), the consistent patterns of parameter influences across different powder additives provide valuable comparative insights. The identified contributions of discharge current, pulse on time, and powder concentration to MRR and SR outcomes establish a foundation for understanding process dynamics, even as they highlight the complex and sometimes stochastic nature of the PMEDM process with novel powder additives.

This study is the first in the literature to comprehensively evaluate the simultaneous effects of both hydroxyapatite (HA) and hexagonal boron nitride (hBN) nanoparticles—used individually and in combination as powder-mixed additives during the PMEDM process—on both machinability and biological properties of Ti6Al4V alloy surfaces. While previous research has typically focused on a single additive, this work directly compares the individual and synergistic impacts of both nanoparticles under identical experimental conditions. Our findings clearly demonstrate that HA/hBN combination not only enhances mechanical properties, but also significantly improves antibacterial surface characteristics, suggesting a new strategy for implant surface design. Furthermore, this interdisciplinary approach provides a valuable contribution to the literature by paving the way for the optimization of surface properties using novel nanoparticle combinations in PMEDM processes for biomedical applications.

Based on our findings, Ti6Al4V alloys modified via PMEDM with HA/hBN powder mixtures are especially promising for orthopaedic, biomedical and dental implant applications where both enhanced mechanical properties and antibacterial performance are critical. The observed improvements in surface hardness and reduction in bacterial biofilm adherence suggest that this technique could be effectively applied to next-generation biomedical devices, as well as metallic surgical instruments where infection control and wear resistance are required. Further studies focusing on in vivo performance and long-term durability are recommended to advance clinical translation. In essence, this study not only elucidates the pivotal parameters affecting PMEDM performance but also offers insights into the manipulation of surface properties to regulate biofilm formation, thereby contributing valuable perspectives to the field of EDM and surface engineering. The results obtained from this study indicate that combining HA and hBN as dielectric additives in PMEDM can improve both surface mechanical characteristics and antibacterial resistance, potentially informing future optimization efforts for biomedical implant surfaces.

Abbreviations

PMEDM	Powder-mixed electrical discharge
HA	Hydroxyapatite
hBN	Hexagonal boron nitride
MRR	Material removal rate
SR	Surface roughness
XRD	X-ray diffraction
SEM	Scanning electron microscopy
EDS	Energy dispersive spectroscopy

Acknowledgements

The author(s) would like to acknowledge funding from the Kırsehir Ahi Evran University, Turkey Scientific Research Projects Coordination Unit under research Grant No. **MMF.A4.22.023.** Authors would like to thank Petek Kartalkanat from KUANTEMET Medikal for her support in this study. The author(s) also thank Kütahya Dumlupınar University Advanced Technologies Center (ILTEM) for their valuable assistance.

Data availability

The data that support the findings of this study are available on request from the corresponding author.

Declarations

Conflict of interest The author(s) declared no potential conflicts of interest with respect to research, authorship and/or publication of this article.

References

[1] Bloyce A, Qi P Y, Dong H and Bell T 1998 Surface modification of titanium alloys for combined improvements in corrosion and wear resistance. *Surf. Coatings Technol.* 107: 125–132.

[2] Geetha M, Singh A K, Asokamani R and Gogia A K 2009 Ti based biomaterials, the ultimate choice for orthopaedic implants - A review. *Prog. Mater. Sci.* 54: 397–425.

[3] Niinomi M, Nakai M and Hieda J 2012 Development of new metallic alloys for biomedical applications. *Acta Biomater.* 8: 3888–3903.

[4] Zhang L C and Chen L Y 2019 A review on biomedical titanium alloys: recent progress and prospect. *Adv. Eng. Mater.* 21: 1–29.

[5] Sarraf M, Rezvani Ghomi E, Alipour S, Ramakrishna S and Liana Sukiman N 2022 A state-of-the-art review of the fabrication and characteristics of titanium and its alloys for biomedical applications. *Bio-Design Manuf.* 5: 371–395.

[6] Kang L M and Yang C 2019 A review on high-strength titanium alloys: microstructure, strengthening, and properties. *Adv. Eng. Mater.* 21: 1–27.

[7] Hsu H C, Wong K K, Wu S C, Chen Y X and Ho W F 2022 Metastable dual-phase Ti–Nb–Sn–Zr and Ti–Nb–Sn–Fe alloys with high strength-to-modulus ratio. *Mater. Today Commun.* 30: 103168.

[8] Keles Dayauc A 2024 The electrochemical and tribological behavior of carbide and carbonitride films in bio-simulated fluid. *Int. J. Refract. Met. Hard Mater.* 124: 106827.

[9] Jabbaripour B, Sadeghi M H, Faridvand S and Shabgard M R 2012 Investigating the effects of edm parameters on surface integrity, mrr and twr in machining of Ti-6Al-4V. *Mach. Sci. Technol.* 16: 419–444.

[10] Singh V, Katyal P, Kumar K and Kumar R 2022 Surface integrity and biological response of Ti-Alloy implants after surface modification. *Mater. Today Proc.* 56: 2451–2468.

[11] Mohanty S, Das A K and Dixit A R 2022 Surface integrity of tribo-adaptive layer prepared on Ti6Al4V through μEDC process. *Surf. Coatings Technol.* 429: 127922.

[12] Kumar A, Sijina K P, Rajanikant G K and Kuriachen B 2022 Experimental investigation into the effects of electric discharge surface modification process parameters on the biocompatibility of Ti6Al4V. *Biomed. Eng. Adv.* 4: 100063.

[13] Al-Amin M, Abdul Rani A M, Abdu Aliyu A A, Abdul Razak M A, Hastuty S and Bryant M G 2020 Powder mixed-EDM for potential biomedical applications: a critical review. *Mater. Manuf. Process.* 35: 1789–1811.

[14] Ishfaq K, Maqsood M A, Anwar S, Harris M, Alfaify A and Zia A W 2022 EDM of Ti6Al4V under nano-graphene mixed dielectric: a detailed roughness analysis. *Int. J. Adv. Manuf. Technol.* 120: 7375–7388.

[15] Ekmekci N and Efe Y 2022 The effect of nano and micro hydroxyapatite powder additives on surface integrity in electrical discharge machining of Ti6Al4V alloy. *Surf. Coatings Technol.* 445: 128708.

[16] Mahajan A, Devgan S and Sidhu S S 2021 Surface alteration of biomedical alloys by electrical discharge treatment for enhancing the electrochemical corrosion, tribological and biological performances *Surf. Coatings Technol.* 405: 126583.

[17] Anbuchezhiyan G, Saravanan R, Pugazhenthi R, Palani K and Mamidi V K 2022 Influence of coated electrode in nanopowder mixed EDM of Al-Zn-Mg-Si3N4Composite. *Adv. Mater. Sci. Eng.* 2022: 9539790.

[18] Chaudhari R, Khanna S, Patel V K, Vora J, Plaza S and de Lacalle L N L 2023 Experimental investigations of using aluminum oxide (Al_2O_3) and nano-graphene powder in the electrical discharge machining of titanium alloy. *Micromachines* 14: 2247.

[19] Baroi B K, Jagadish F and Patowari P K 2024 Effect of boric acid in powder mixed EDM of Ti-6al-4V ELI. *Mater. Manuf. Process.* 39: 130–143.

[20] Yoda I, Koseki H, Tomita M, Shida T, Horiuchi H, Sakoda H and Osaki M 2014 Effect of surface roughness of biomaterials on Staphylococcus epidermidis adhesion. *BMC Microbiol.* 14: 1–7.

[21] Wang Y H, Liao C C, Chen Y C, Ou S F and Chiu C Y 2020 The feasibility of eco-friendly electrical discharge machining for surface modification of Ti: a comparison study in surface properties, bioactivity, and cytocompatibility. *Mater. Sci. Eng. C* 108: 110192.

[22] Bisaria H, Bhusan Patra B and Mohanty S 2022 Surface modification during hydroxyapatite powder mixed electric discharge machining of metallic biomaterials: a review. *Surf. Eng.* 38: 680–706.

[23] Bui V D, Mwangi J W and Schubert A 2019 Powder mixed electrical discharge machining for antibacterial coating on titanium implant surfaces. *J. Manuf. Process.* 44: 261–270.

[24] Opoz T, Yasar H, Murphy M, Ekmekci N and Ekmekci B 2019 Ti6Al4V surface modification by hydroxyapatite powder mixed electrical discharge machining for medical applications. *Int. J. Adv. Eng. Pure Sci.* 31: 1–10.

[25] Bains P S, Bahraminasab M, Sidhu S S and Singh G 2020 On the machinability and properties of Ti–6Al–4V biomaterial with n-HAp powder–mixed ED machining. *Proc. Inst. Mech. Eng. Part H J. Eng. Med.* 234: 232–242.

[26] Nauryz N, Omarov S, Kenessova A, Pham T T, Talamona D and Perveen A 2023 Powder-mixed micro-electro-discharge machining-induced surface modification of titanium alloy for antibacterial properties. *J. Manuf. Mater. Process.* 7(6): 214.

[27] Saurabh S, Kumar A and Roy B K 2023 Investigation of surface integrity of Ti-6Al-4V using graphite nanopowder mixed electrical discharge machining. *J. Mater. Eng. Perform.* 33: 11957–11967.

[28] Sharma D, Mohanty S and Das A K 2020 Surface modification of titanium alloy using hBN powder mixed dielectric through micro-electric discharge machining. *Surf. Coatings Technol.* 381: 125157.

[29] Devgan S and Sidhu S S 2020 Surface modification of β-type titanium with multi-walled CNTs/ μ-HAp powder mixed electro discharge treatment process. *Mater. Chem. Phys.* 239: 122005.

[30] Urtekin L, Şahin İB, Yılan F, Kuloğlu E and Genç A 2024 Investigation and optimization of cutting performance of high chrome white cast iron by wire erosion. *Arab. J. Sci. Eng.* 49: 1585–1596.

[31] Kolli M and Kumar A 2015 Effect of dielectric fluid with surfactant and graphite powder on Electrical Discharge Machining of titanium alloy using Taguchi method. *Eng. Sci. Technol. Int. J.* 18: 524–535.

[32] Mhatre M S, Sapkal S U and Pawade R S 2014 Electro discharge machining characteristics of Ti-6Al-4V alloy: a grey relational optimization. *Procedia Mater. Sci.* 5: 2014–2022.

[33] Şahin İB, Yilan F and Urtekin L 2023 Optimisation on machining parametres by EDM of TiN coated Ti6Al4V alloys. *Adv. Mater. Process. Technol.* 10: 960–970.

[34] Al-Amin M, Abdul-Rani A M, Danish M, Zohura F T, Rubaiee S, Ahmed R, Ali S and Sarikaya M 2021 Analysis of hybrid HA/CNT suspended-EDM process and multiple-objectives optimization to improve machining responses of 316L steel. *J. Mater. Res. Technol.* 15: 2557–2574.

[35] Barot R S, Valaki J B, Makwana A H and Beravala H 2022 *Experimental Investigation and Machinability Study of Ni–Cr-Based Super Alloy Using Powder Mixed EDM* (Springer Singapore)

[36] Çavdar F, Yildiz C and Kanca E 2023 Response surface modeling of material removal and tool wear rate in powder mixed electrical discharge machining of CoCrMo alloy. *J. Mater. Mechatron. A* 4: 571–587.

[37] Davis R, Singh A, Debnath K, Soares P, Och S H, Keshri A K, Sopchenski L and Terryn H A 2023 Enhanced abrasive-mixed-μ-EDM performance towards improved surface characteristics of biodegradable Mg AZ31B alloy. *Int. J. Adv. Manuf. Technol.* 124: 2685–2700.

[38] Dewan P R and Kundu P K 2024 Optimization of parameters of powder added EDM of Nimonic C-263 using TOPSIS. *Sadhana – Acad. Proc. Eng. Sci.* 49: 190.

[39] Koseki H, Yonekura A, Shida T, Yoda I, Horiuchi H, Morinaga Y, Yanagihara K, Sakoda H, Osaki M and Tomita M 2014 Early staphylococcal biofilm formation on solid orthopaedic implant materials: In vitro study. *PLoS One* 9: 1–8.

[40] Urtekin L, Aydin Ş, Sevim A, Gök K and Uslan I 2022 Experimental determination of biofilm and mechanical properties of surfaces obtained by co2laser gas-assisted nitriding of Ti-6Al-4V alloy. *Surf. Rev. Lett.* 29: 1–11.

[41] Ekmekci B and Ersöz Y 2012 How suspended particles affect surface morphology in powder mixed electrical discharge machining (PMEDM). *Metall. Mater. Trans. B Process Metall. Mater. Process. Sci.* 43: 1138–1148.

[42] Rahul, Mishra D K, Datta S and Masanta M 2018 Effects of tool electrode on EDM performance of Ti-6Al-4V. *Silicon* 10: 2263–2277.

[43] Zhang W, Li L, Wang N, Meng J and Ren J 2022 Surface modification of Ti-6Al-4 V by gas–liquid mixed EDM. *Int. J. Adv. Manuf. Technol.* 119: 3833–3844.

[44] Kirubagharan R, Dhanabalan S and Karthikeyan T 2024 The effect of electrode size on performance measures of inconel X750 using nano-SiC powder mixing electrical discharge machining. *J. Mater. Eng. Perform.* 33: 1283–1303.